Chapter-4

Laser Applications

4.1 Spatial frequency filtering

4.1.1 Fourier transforming property of the lens and spatial frequencies*

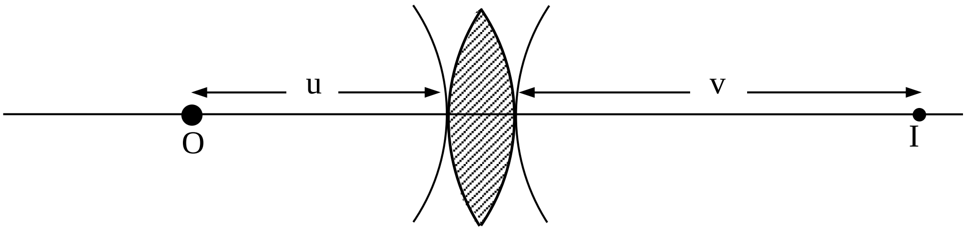

The coordinate of any point on the object plane (perpendicular to the axis of the lens) is given by, (x, y, –u), then

$$r = \left(x^2+y^2+u^2\right)^{1/2} = u\left(1+\frac{x^2+y^2}{u^2}\right)^{1/2} \approx u\left(1+\frac{x^2+y^2}{2u^2}\right) \approx \left(u+\frac{x^2+y^2}{2u}\right)$$

Then phase of the incident diverging spherical wave is given by,

$$e^{-ikr_1} \approx e^{-ik\left(u+\frac{x^2+y^2}{2u}\right)} = e^{-iku-ik\left(\frac{x^2+y^2}{2u}\right)} = e^{-iku}e^{-ik\left(\frac{x^2+y^2}{2u}\right)} \qquad (1)$$

Similarly, the phase of the converging wave at the image plane is,

$$e^{ikr_2} \approx e^{ikv}e^{ik\left(\frac{x^2+y^2}{2v}\right)} \qquad (2)$$

Let the effect of the lens on the field distribution when refraction takes place is denoted by p_L.

Then from eqns.1 and 2, $\quad p_L e^{-ikr_1} = e^{ikr_2}$

$$p_L = \frac{e^{ikr_2}}{e^{-ikr_1}} = \frac{e^{ikv}e^{ik\left(\frac{x^2+y^2}{2v}\right)}}{e^{-iku}e^{-ik\left(\frac{x^2+y^2}{2u}\right)}} = e^{ik(u+v)}e^{\frac{ik}{2}\left(x^2+y^2\right)\left(\frac{1}{u}+\frac{1}{v}\right)} = e^{\frac{ik}{2f}\left(x^2+y^2\right)} \qquad (3)$$

Since $e^{ik(u+v)}$ is a constant phase factor and can be taken as unity.

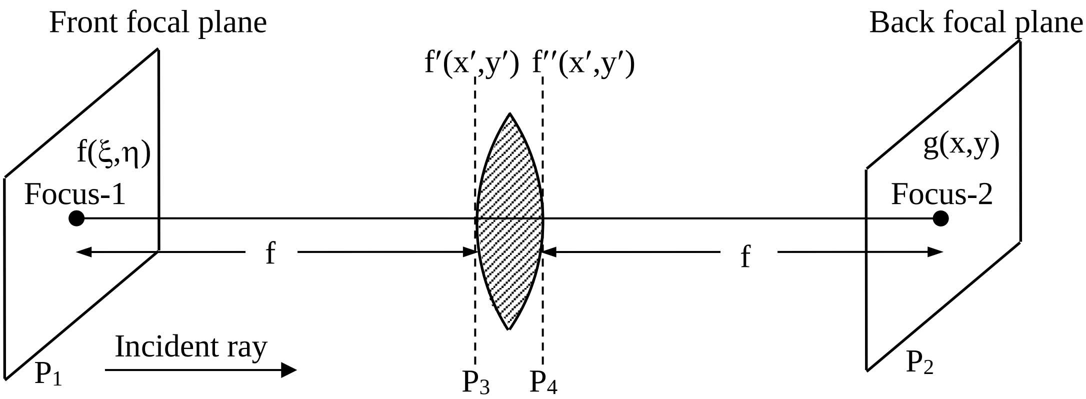

By eqn.4 of sec.1.10 we have,

$$g(x, y, z) \approx \frac{i}{\lambda z}e^{-ikz}\iint f\left(x', y'\right)e^{-\frac{ik}{2z}\left[\left(x-x'\right)^2+\left(y-y'\right)^2\right]}dx'dy' \qquad (4)$$

where, $f(x', y')$ is the field distribution on the plane at z = 0 and g(x, y , z) is the field at the point (x, y, z).

Let f(ξ, η) be the field distribution at the front focal plane where z = 0 (origin of the coordinate system at focus-1). Then the field distribution at any point on the plane P_3, $f'(x', y')$ is given by eqn.4 (change $x' \to \xi$, $y' \to \eta$, z = f and $x \to x'$, $y \to y'$, z = 0),

$$f'(x', y', f) = \frac{i}{\lambda f} e^{-ikf} \iint f(\xi, \eta) e^{-\frac{ik}{2z}\left[(x'-\xi)^2+(y'-\eta)^2\right]} d\xi d\eta \qquad (5)$$

After passing through the prism, the field distribution at the plane P_4 is given by (since x, y and z remain same),

$$f''(x', y', f) = p_L f'(x', y', f) = \frac{i}{\lambda f} e^{-ikf} \iint f(\xi, \eta) e^{-\frac{ik}{2z}\left[(x'-\xi)^2+(y'-\eta)^2\right]} e^{\frac{ik}{2f}\left(x'^2+y'^2\right)} d\xi d\eta \qquad (6)$$

Finally, the field distribution at the back focal plane is obtained by using eqn.4 once again,

$$g(x, y) = g(x, y, z{:}2f) = \frac{i}{\lambda f} e^{-ikf} \iint f''(x', y', f) e^{-\frac{ik}{2f}\left[(x-x')^2+(y-y')^2\right]} dx'dy'$$

$$= \frac{i}{\lambda f} e^{-ikf} \iint \frac{i}{\lambda f} e^{-ikf} \iint f(\xi, \eta) e^{-\frac{ik}{2f}\left[(x'-\xi)^2+(y'-\eta)^2\right]} e^{\frac{ik}{2f}\left(x'^2+y'^2\right)} d\xi d\eta e^{-\frac{ik}{2f}\left[(x-x')^2+(y-y')^2\right]} dx'dy'$$

$$= \left(\frac{i}{\lambda f}\right)^2 e^{-2ikf} \iint\iint f(\xi, \eta) e^{-\frac{ik}{2f}\left[(x'-\xi)^2+(y'-\eta)^2\right]} e^{-\frac{ik}{2f}\left[(x-x')^2+(y-y')^2\right]} e^{\frac{ik}{2f}\left(x'^2+y'^2\right)} d\xi d\eta dx'dy'$$

$$= \left(\frac{i}{\lambda f}\right)^2 e^{-2ikf} e^{-\frac{ik}{2f}\left[x^2+y^2\right]} \iint\iint d\xi d\eta\, f(\xi, \eta) e^{-\frac{ik}{2f}\left[\xi^2+\eta^2\right]} e^{-\frac{ik}{2f}\left[x'^2-2x'(x+\xi)\right]} dx' e^{-\frac{ik}{2f}\left[y'^2-2y'(\eta+y)\right]} dy'$$

Using the standard integral, $\int_{-\infty}^{\infty} e^{-px^2+qx} dx = \left(\frac{\pi}{p}\right)^{1/2} e^{\frac{q^2}{4p}}$

$$= \left(\frac{i}{\lambda f}\right)^2 e^{-2ikf} e^{-\frac{ik}{2f}\left[x^2+y^2\right]} \iint d\xi d\eta\, f(\xi, \eta) e^{-\frac{ik}{2f}\left[\xi^2+\eta^2\right]} \left(\frac{2\pi f}{ik}\right) e^{\frac{ik}{2f}(x+\xi)^2} e^{\frac{ik}{2f}(\eta+y)^2}$$

$$= \left(\frac{i}{\lambda f}\right)^2 \left(\frac{2\pi f}{ik}\right) e^{-2ikf} \iint d\xi d\eta\, f(\xi, \eta) e^{\frac{ik}{f}(x\xi+y\eta)}$$

$$= \frac{i}{\lambda f} e^{-2ikf} \iint f(\xi, \eta) e^{2\pi i\left(\frac{x\xi}{\lambda f}+\frac{y\eta}{\lambda f}\right)} d\xi d\eta \qquad (7)$$

Thus, apart from the constant phase factor e^{-2ikf}, the amplitude distribution at the back focal plane of a lens is the Fourier transform of the amplitude distribution at the front focal plane evaluated at the *spatial frequencies* $\frac{x}{\lambda f}$ and $\frac{y}{\lambda f}$. [We know that $e^{i\omega t} = e^{i2\pi ft}$ is periodic in time. Similarly, the terms in eqn.7 is periodic in space x and y].

4.1.2 Spatial frequency filtering

Spatial frequency is a characteristic of any structure that is periodic across position in space. It is a measure of how often sinusoidal components of the structure repeat per unit distance. The SI unit of it is the cycles per metre.

We have already seen that the Fourier transform of a time dependent periodic function can be written in the following form,

$$g(\omega) = \frac{1}{(2\pi)^{1/2}}\int_{-\infty}^{\infty} f(t')e^{i\omega t'}dt' \quad (1a)$$

And,
$$f(t) = \frac{1}{(2\pi)^{1/2}}\int_{-\infty}^{\infty} g(\omega)e^{-i\omega t}d\omega \quad (1b)$$

where, ω represents the angular frequency.

Just as the Fourier transform of a time varying signal gives its temporal frequency spectrum, similarly the spatial Fourier transform of a spatially varying function (like the transmittance of an object) gives the spatial frequency spectrum of the function. By eqn.7 we have seen that the field distribution produced in the back focal plane of an aberrationless converging lens is the two-dimensional Fourier transform of the field distribution in the front focal plane of the lens.

If $f(x', y')$ represents the object distribution in the front focal plane of the converging lens, then the field distribution in the back focal plane is given by (in eqn.7 sec.2.7.1 change $\xi \to x'$ and $\eta \to y'$ and without considering the constant phase factor e^{-2ikf}),

$$g(x, y) = \frac{i}{\lambda f}\iint f(x', y')e^{2\pi i\left(\frac{xx'}{\lambda f}+\frac{yy'}{\lambda f}\right)}dx'dy' \quad (2a)$$

$$= \frac{i}{\lambda f}F\left(\frac{x}{\lambda f}, \frac{y}{\lambda f}\right) \quad (2b)$$

where, $F\left(\frac{x}{\lambda f}, \frac{y}{\lambda f}\right)$ is the Fourier transform of f(x, y) evaluated at the spatial frequencies $\frac{x}{\lambda f}$ and $\frac{y}{\lambda f}$. Here, f is the focal length of the lens and λ is the wavelength of the light used for illuminating the object. Let an object with space varying transmittance is placed at the front focal plane of the lens. Let the transmittance of the object be in the form,

$$f(x', y') = A\cos\left(\frac{2\pi x'}{a}\right) = \frac{A}{2}\left[e^{i\frac{2\pi x'}{a}} + e^{-i\frac{2\pi x'}{a}}\right] \quad (3)$$

Then the corresponding field distribution at the back focal plane is,

$$g(x, y) = \frac{iA}{2\lambda f}\iint\left[e^{i\frac{2\pi x'}{a}} + e^{-i\frac{2\pi x'}{a}}\right]e^{2\pi i\left(\frac{xx'}{\lambda f}+\frac{yy'}{\lambda f}\right)}dx'dy'$$

$$= \frac{iA}{2\lambda f}\left[\iint e^{i\frac{2\pi x'}{a}}e^{2\pi i\left(\frac{xx'}{\lambda f}+\frac{yy'}{\lambda f}\right)}dx'dy' + \iint e^{-i\frac{2\pi x'}{a}}e^{2\pi i\left(\frac{xx'}{\lambda f}+\frac{yy'}{\lambda f}\right)}dx'dy'\right] \quad (4)$$

$$= \frac{iA}{2\lambda f}\left[\int e^{2\pi i x'\left(\frac{x}{\lambda f}+\frac{1}{a}\right)}dx'\int e^{2\pi i\left(\frac{yy'}{\lambda f}\right)}dy' + \int e^{2\pi i x'\left(\frac{x}{\lambda f}-\frac{1}{a}\right)}dx'\int e^{2\pi i\left(\frac{yy'}{\lambda f}\right)}dy'\right]$$

[Now we use the following two properties of Dirac delta function.

1. We can express the delta function as a Fourier transform as given by,

$$\delta(x) = \frac{1}{2\pi}\int_{-\infty}^{+\infty} e^{ikx}dk$$

2. $$\delta(ax) = \frac{1}{a}\delta(x)$$]

Then, $$g(x, y) = \frac{iA}{2\lambda f}\left[\delta\left(\frac{x}{\lambda f}+\frac{1}{a}\right)+\delta\left(\frac{x}{\lambda f}-\frac{1}{a}\right)\right]\delta(y) \tag{5}$$

where, $\delta\left(\frac{x}{\lambda f}+\frac{1}{a}\right) = \int e^{2\pi i x'\left(\frac{x}{\lambda f}+\frac{1}{a}\right)}dx'$ is the Fourier transform of $e^{i\frac{2\pi x'}{a}}$, $\delta\left(\frac{x}{\lambda f}-\frac{1}{a}\right) = \int e^{2\pi i x'\left(\frac{x}{\lambda f}-\frac{1}{a}\right)}dx'$ and $\delta(y) = \int e^{2\pi i\left(\frac{yy'}{\lambda f}\right)}dy'$. Eqn.5 represents the field corresponding to two bright dots at $\left(x=\frac{\lambda f}{a},\ y=0\right)$ and $\left(x=-\frac{\lambda f}{a},\ y=0\right)$. (6)

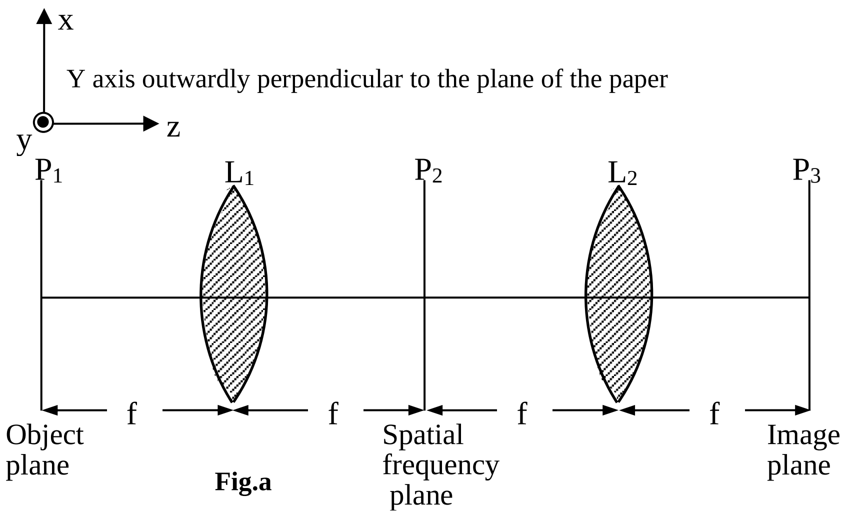

Fig.a

It can be shown that the Fourier transform of the Fourier transform of a function is the original function with an inversion. That is,

$$\mathcal{F}[\mathcal{F}\{f(x)\}] = f(-x) \tag{7}$$

Thus, if another converging lens L_2 is placed such that its front focal plane coincides with the back focal plane of the first lens L_1, then one would obtain the original object distribution with an inversion at the back focal plane P_3 of L_2. The resultant field distribution on the plane P_3 can be controlled suitably by placing apertures on the back plane P_2 of the first lens and hence one can perform operations on the spatial frequency spectrum of the object. The various apertures,

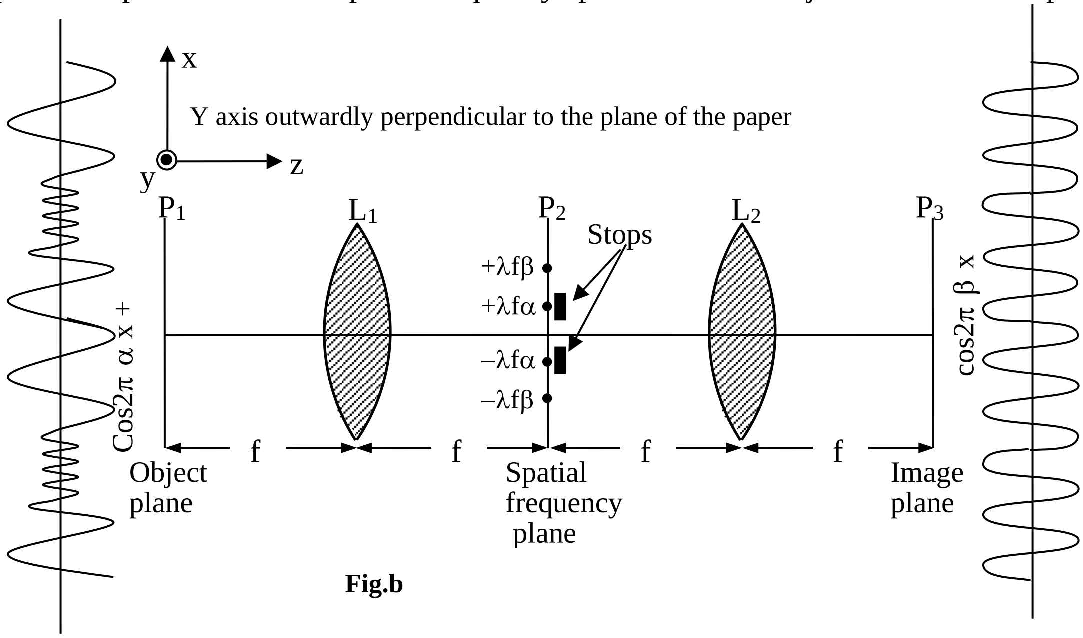

Fig.b

stops, etc. that are placed at the plane P_2 to filter the spatial frequencies are called *filters* and the process is known as *spatial frequency filtering*.

A *low-pass filter* allows the low spatial frequencies to pass through it and blocks the high spatial frequencies. This could be a screen with a small hole at the axis of the system. Similarly a *high-pass filter* allows high spatial frequencies and blocks the low spatial frequencies. There are also *complex filters* that can alter both the amplitude and phase of the various spatial frequency components of the image.

As an example, let us consider an object with an amplitude variation of the form,

$$f(x') = A\cos(2\pi\alpha x') + B\cos(2\pi\beta x')$$

Comparing with eqns.3 and 6 we see that one would obtain 4 spots at $x = +\lambda f\alpha$, $+\lambda f\beta$, $-\lambda f\alpha$ and $-\lambda f\beta$ as shown in fig.b. If no stops are used one obtains the same amplitude distribution in plane P_3 as that in the plane P_1. If two stops are used at the points $+\lambda f\alpha$ and $-\lambda f\alpha$ such that no light from these points reach the lens L_2, one obtains a field distribution proportional to $\cos(2\pi\beta x)$. Thus, by placing the stops in the plane P_2 we can filter out the frequency component α. This is the *basic principle behind spatial frequency filtering*.

Applications of spatial frequency filtering: Now we see some of the applications of spatial frequency filtering.

1. One can see that a newspaper photograph is made up of a large number of closely arranged dots. These closely arranged dots represent the high spatial frequency while the general image formed by these dots represents low frequency components. The dots due to high frequency components can be got rid of by spatial frequency filtering. The fig.a shows a photograph which consists of regularly placed black and white squares. (All spatial frequencies present). The spatial frequency spectrum of the object is shown in the fig.b. If we place a screen with a small hole at the centre on the back focal plane of lens L_1, the image produced is devoid of these dot patterns as shown in the fig.c. By placing the screen with small hole, one has filtered out the high frequency components in the object.

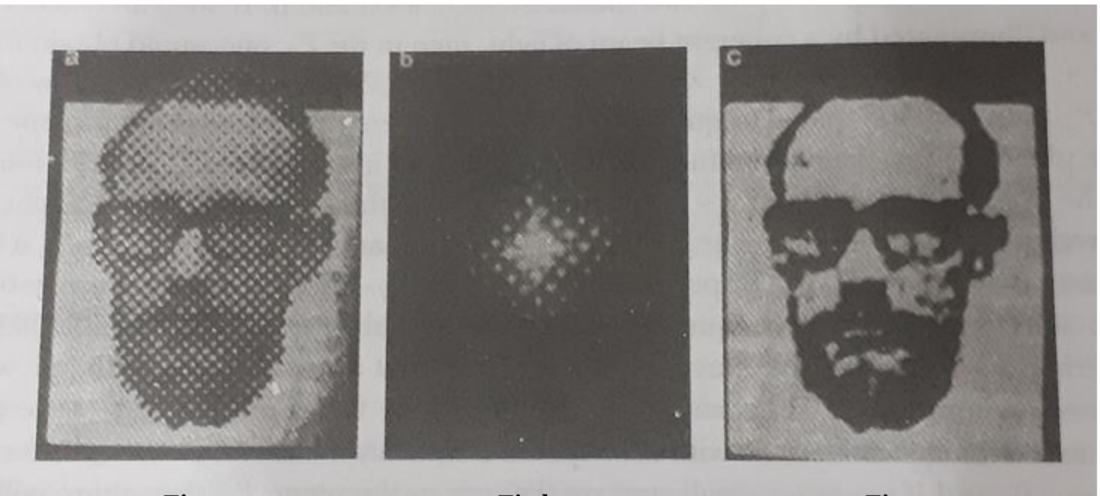

Fig.a **Fig.b** **Fig.c**

A photograph consisting of regularly spaced array of black and white squares is shown in fig.a. The corresponding spatial frequency spectrum which appears on the plane P_2 is shown in fig.b. If a pinhole is placed in the back focal plane P_2 to block off high frequency components an image of the form as shown in fig.c is obtained. Note that the missing part of the eyeglass frame is visible now.

2. Another application of spatial frequency filtering is in *contrast enhancement*. When the background light is very large the contrast in the image is poor. The background light

represents the distribution of zero spatial frequency. If small stop is placed on the axis at the back focal plane of lens L_1 to cut off the low frequency components we obtain on the back focal plane of lens L_2 an image with much better contrast. Such a process is termed as contrast enhancement.

3. Spatial frequency filtering can also be used for detecting non-periodic errors in a periodic structure. This can be done in two ways. One could either allow transmitting all the spatial frequencies corresponding to the periodic array and stops most of the light from the random noise (due to the defects) or to transmit all frequencies corresponding to the defects and blocks all the frequencies that correspond to the periodic arrays. Such techniques have been used in photo mask inspection, electron tube grid inspection, etc.
4. Another important application of spatial frequency filtering is in character recognition problems where it is necessary to detect the presence of certain characters in an optical image. The complex filters produced using holographic principles are used for this purpose. The output of the optical system is such that if there is a matching with desired character one obtains a bright spot of light in the image. Figure shows the identification of a fingerprint by this technique. The top figure is the case of fingerprints that are matched and a bright spot of light is formed. If the fingerprints do not match instead of bright spot only a smear is formed as shown in the lower figure. Character recognition problems will also find application in military defence, where it is necessary to identify certain objects of interest.

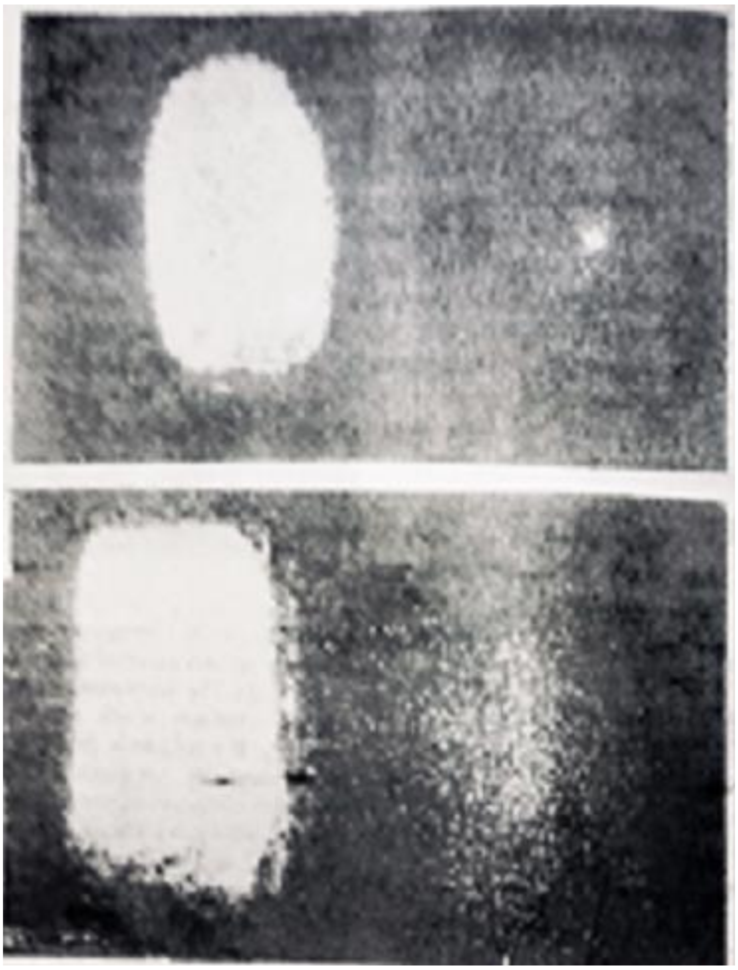

5. Image deblurring is another application of spatial frequency filtering. Let $f(x,y)$ represent the image of an object. An image may get blurred during photography due to the movement of the camera or it is out of focus. In this case we get an image $g(x,y)$ instead of $f(x,y)$. In terms of the intensity distribution $f(x',y')$ of the object we can write the intensity distribution of the blurred image as,

$$\begin{aligned} g(x,y) &= \iint f(x',y')\, h(x-x', y-y')\,dx'dy' \\ &= f(x,y) * h(x,y) \qquad (1) \end{aligned}$$

where, $h(x,y)$ is the intensity distribution of the blurred image and the * (star) represents the convolution. If we assume that the transmittance of the exposed film to be proportional to $g(x,y)$, then the amplitude transmittance of the recorded film would be proportional to $g(x,y)$. If we place this film in the front focal plane of a lens and illuminate by a normally incident laser beam, then the amplitude distribution on the back focal plane would be the Fourier transform of $g(x,y)$. We can write it as,

$$\mathcal{F}\{g(x,y)\} = G\left(\frac{x}{\lambda f},\frac{y}{\lambda f}\right) = G(u,v) \tag{2}$$

where, $u=\frac{x}{\lambda f}$ and $v=\frac{y}{\lambda f}$ are the spatial frequencies. Since the Fourier transform of the convolution of two functions is the product of their Fourier transforms, we can write,

$$\mathcal{F}\{g(x,y)\} = \mathcal{F}\{f(x,y)*h(x,y)\} = \mathcal{F}\{f(x,y)\}\mathcal{F}\{h(x,y)\} \tag{3}$$

i.e. $$G(u,v) = F(u,v)H(u,v) \tag{4}$$

If we place a filter whose transmittance is proportional to $\frac{1}{H(u,v)}$ on the back focal plane of the lens, then the filtered spectrum would be $G(u,v).\frac{1}{H(u,v)}$. Then by eqn.4 we get,

$$G(u,v).\frac{1}{H(u,v)} = F(u,v) \tag{5}$$

Now using a second lens we can Fourier transform the filtered spectrum further to produce the deblurred image $f(x,y)$. The filter whose transmittance equal to $\frac{1}{H(u,v)}$ can be generated approximately using holographic principles. Fig.a shows the blurred image and fig.b shows the deblurred image after optical deblurring.

Figa

Figb

4.2 Holography

The term holography comes from the Greek meaning '*whole writing*'. It is different from ordinary photograph, which represents only a two-dimensional recording of a three-dimensional object. A photograph is obtained by recording the intensity distribution that prevailed at the plane of photographic film when it was exposed. The light sensitive medium is sensitive to the intensity distribution. In an ordinary photograph the phase distribution of the waves coming from the three-dimensional object cannot be recorded. So, the three-dimensional character of the object is lost in the photograph.

Holography is a method in which one records not only the amplitudes but also the phases of the light waves from the object. The principles of holography were first put forward by Dennis

Gabor, of the Imperial College of Science and Technology, University of London in 1947 (published in 1948) and became further developed after the invention of laser in 1960. He has been awarded Nobel Prize in 1971 for his '*three dimensional lensless method of photography (Holography).*

Principle: Holography is a two-step process by which (1) an object is illuminated by coherent light is made to produce interference fringes in a photosensitive medium, such as a photographic emulsion and (2) re-illumination of the developed interference pattern by light of same wavelength produces a three dimensional image of the original object.

Step-1: Recording of hologram: Dennis Gabor proposed a method of recording not only the amplitudes but also the phases of the light waves from the object. During the recording process the light waves emanating from the object are superimposed with another coherent wave called the reference wave. These two waves interfere in the plane of the recording medium and produce interference fringes. This process is known as recording process. The recording medium records the intensity distribution of the interference pattern which is a characteristic of the object.

The field produced by the object wave in the plane of the recording medium is represented by,

$$O(x, y) = O_0(x, y)e^{i\varphi(x,y)} \quad (1)$$

where, $O_0(x, y)$ is the amplitude part and $\varphi(x, y)$ is the phase part. (Since we need only the amplitude the time dependence $e^{-i\omega t}$ is not considered here). Similarly, the field produced by the reference wave in the plane of the recording medium is,

$$R(x, y) = Ae^{i\psi(x,y)} \quad (2)$$

The amplitude of the obliquely incident reference wave can be taken as constant. Therefore, the total field produced at the recording medium is,

$$U(x, y) = O_0(x, y)e^{i\varphi(x,y)} + Ae^{i\psi(x,y)} \quad (3)$$

Then the intensity pattern recorded by the recording medium,

$$\begin{aligned} I(x, y) &= \left|U(x, y)\right|^2 = \left\{O_0(x, y)e^{i\varphi(x,y)} + Ae^{i\psi(x,y)}\right\}^* \left\{O_0(x, y)e^{i\varphi(x,y)} + Ae^{i\psi(x,y)}\right\} \\ &= \left\{O_0(x, y)e^{-i\varphi(x,y)} + Ae^{-i\psi(x,y)}\right\}\left\{O_0(x, y)e^{i\varphi(x,y)} + Ae^{i\psi(x,y)}\right\} \\ &= O_0^2(x, y) + O_0(x, y)Ae^{-i\varphi(x,y)}e^{i\psi(x,y)} + O_0(x, y)Ae^{-i\psi(x,y)}e^{i\varphi(x,y)} + A^2 \\ &= O_0^2(x, y) + A^2 + O_0(x, y)Ae^{i\{\varphi(x,y)-\psi(x,y)\}} + O_0(x, y)Ae^{-i\{\varphi(x,y)-\psi(x,y)\}} \quad (4a) \\ &= O_0^2(x, y) + A^2 + 2O_0(x, y)A\cos\{\varphi(x,y) - \psi(x,y)\} \quad (4b) \end{aligned}$$

Eqn.4 shows that the phase of the object wave is embedded in the intensity distribution. Since the intensity pattern has both the amplitude and phase recorded in it, Gabor called the recording as hologram. In order to record hologram, the light waves from the object is superimposed with a reference wave and the interference pattern is recorded on a photographic plate. The reference wave is usually a plane wave. This recorded interference pattern forms the hologram. It contains information not only about the amplitudes but also about the phases of waves from object. Unlike a photograph the hologram does not resemble with the object. Hologram has in it a coded form of the object wave.

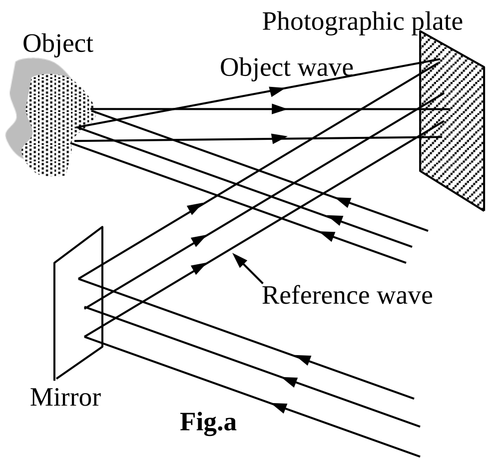

Fig.a

Step-2: Reconstruction or viewing a hologram

To view the image, the hologram is again illuminated with another wave called the reconstruction wave. In most cases the reconstruction wave is identical to the reference wave in all optical respects. The process is known as reconstruction.

In the reconstruction process, there emerges from the hologram various wave components, one of which is the object wave itself. The exposed recording medium is developed such that it has a transparency with a certain transmittance. Under proper conditions, the amplitude transmittance of the hologram can be made to be linearly proportional to $I(x,y)$ given in eqn.4. Thus, apart from some constants, one can write the amplitude transmittance of the hologram as,

$$t(x,y) = I(x,y) \qquad (5)$$

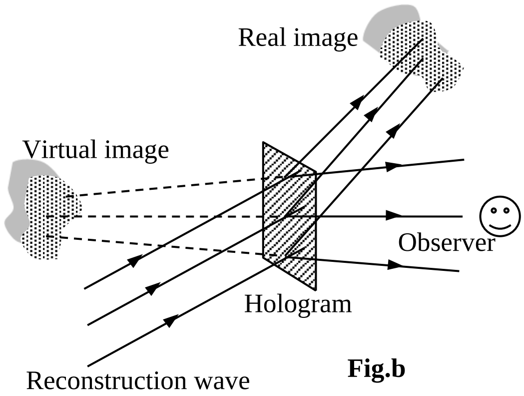

Fig.b

If this hologram is illuminated with the reconstruction wave, the emerging wave is obtained by multiplying the amplitude of the incident wave with amplitude transmittance.

i.e. Amplitude of the emerging wave $= t(x,y)R(x,y)$

Using eqn.2 and 5,

Amplitude of the emerging wave $= I(x,y)Ae^{i\psi(x,y)}$

Using eqn.4a,

Amplitude of the emerging wave

$$= \left[O_0^2(x,y) + A^2 + O_0(x,y)Ae^{i\{\varphi(x,y)-\psi(x,y)\}} + O_0(x,y)Ae^{-i\{\varphi(x,y)-\psi(x,y)\}}\right]Ae^{i\psi(x,y)}$$

$$= \left\{O_0^2(x,y) + A^2\right\}Ae^{i\psi(x,y)} + O_0(x,y)A^2e^{i\varphi(x,y)} + O_0(x,y)A^2e^{-i\{\varphi(x,y)-2\psi(x,y)\}} \qquad (6)$$

Eqn.6 shows that the emerging wave consists of three wave components as explained below. These wave components can be spatially separated by the proper choice of the reference wave.

1. The first term represents the amplitude modulated reconstruction wave itself.
2. Apart from the constant multiplication factor, the second term indeed represents the original object wave. Or, it represents the reproduction of the original object wave. This diverging wave forms the virtual image of the object. The wave is identical to the wave that was emanating from the object when its hologram was being recorded. By viewing this wave one can see the reconstructed virtual image of the object in its true three-dimensional form. Just similar to look around the object from different directions one can view the image from different directions and he gets an impression that he is watching the original object. If the hologram is recorded in its sufficient depth of field one is able to see distinctly the objects that are far away. By placing a lens on the path of the wave one can even form an image of the object on a screen.
3. The third term represents the complex conjugate of the object wave. This converging wave generates the real image that can indeed be photographed by placing a suitable light sensitive medium (like a photographic plate) at the position where the real image is formed.

The hologram mentioned here is a plane hologram. There are other holograms like (1) the thick or volume hologram, which is able to produce multiple scenes from the same photographic emulsion, (2) multiplex hologram, which can be used for producing holographic motion pictures, (3) white light reflection hologram and (4) other holograms, which are produced to achieve special effects. These are produced by using lenses and mirrors and using other holographic images as objects.

In-line and off-axis holography: Before the advent of lasers one had to employ the method of in-line holography as proposed by Gabor. In this method the reference beam is approximately parallel to the object wave and hence the path traversed by both the waves are almost equal. This was required because the existing light sources such as mercury discharge lamps had only small coherence lengths. [*Coherence* is a measure of the correlation that exists between the phases of the wave measured at different points. The coherence of a wave depends on the characteristics of its source. *Temporal coherence* is a measure of the correlation between the phases of a light wave at different points along the direction of propagation. Temporal coherence tells us how monochromatic a source is. *Coherence length* is the propagation distance over which a coherent wave (e.g. an electromagnetic wave) maintains a specified degree of coherence. Waves with wavelength λ and $\lambda + \Delta\lambda$, which at some point in space constructively interfere, will no longer constructively interfere after some optical path length $l_c = \lambda^2/(2\pi\Delta\lambda)$; l_c is called the coherence length. For light with a Lorentzian optical spectrum, the coherence length can be calculated as $L_{coh} = \dfrac{c}{\pi\,\delta\nu}$, where, $\Delta\nu$ is the (full width at half-maximum) linewidth (optical bandwidth). This coherence length is the propagation length after which the magnitude of the coherence function has dropped to the value of 1/e].

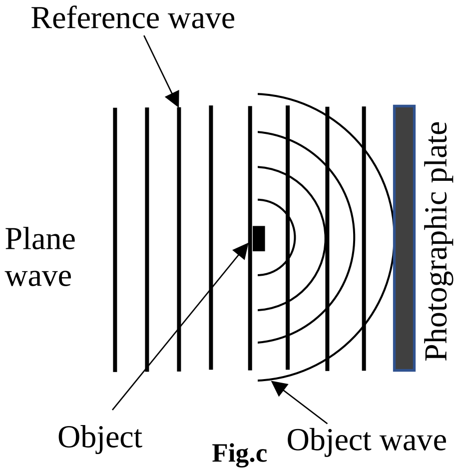

Fig.c

The main disadvantage of in-line holography is that the waves forming virtual and real images also travel along the same direction. Thus, while viewing the virtual image one is faced with an unfocussed real image and conversely.

In the year 1962 Leith and Upatneiks introduced the technique of off-axis holography which overcame the difficulty associated with the in-line technique. In this off-axis method the reference beam is made to fall obliquely on the photographic plate as shown in the fig.a given in sec.4.1.3. If this oblique incidence technique is used in the reconstruction process one obtains well separated virtual and real images. This off-axis technique was made possible by the large coherence length of the laser. The coherence length is very important because holography is essentially an interference phenomenon. Thus, it is essential that the illuminating wave possesses sufficient spatial coherence so that the wave

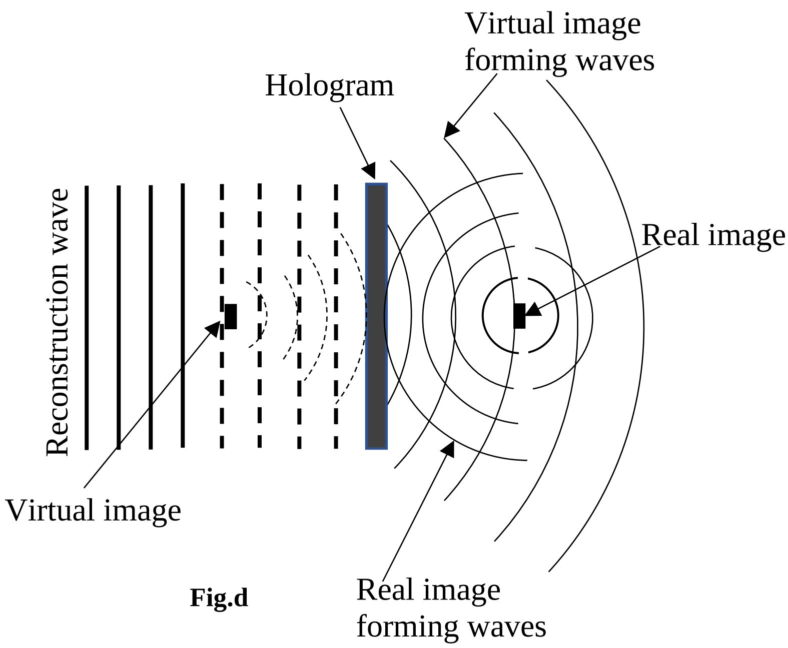

Fig.d

from every point of object may interfere with the reference wave. The stable interference fringes will be formed in the hologram of the complete object scene to be recorded, the maximum path difference between the reference wave and the waves from the object must be less than the coherence length. The wave with sufficient spatial coherence is obtained either by making use of the pinholes for illuminating or to move the source far enough from the scene. Both these methods decrease the available power. The arrival of laser overcame this difficulty.

Important properties (characteristics) of the hologram: One may prefer, at first glance, a photograph rather than a hologram. This is because a photograph shows 'everything clearly' (i.e. information is directly visible) while a hologram is quite unintelligible (i.e. no direct information is visible). However, holograms have some interesting properties which make it preferable to a photograph.

1. The virtual image produced by a hologram appears in complete three-dimensional form. The observer sees something looking very much like the object as it was in the process of hologram recording. If he tilts his head, he notices other objects behind the one in the foreground or he may see new details that were not noticeable before. That is, the image manifests vivid realism.
2. Destruction of a portion of a photographic image results in an irreparable loss of information corresponding to a part of the object while the destruction of a part of the hologram does not erase a specific portion of the image and hence the corresponding part of the object. Even if the hologram is broken into pieces, each part is capable of reconstructing the entire object. This can be explained as follows.

   When one records the hologram of a diffusely reflecting object, each point on the object scatters light on the complete surface of the hologram. Or, every part of the hologram receives light from all parts of the object and therefore contains information about the geometrical characteristics of the image of the entire object. Thus, each part of the hologram, no matter how small, can reproduce the entire image. Consequently, destruction of a part of a hologram does not erase a specific portion of the image. But the resolution of the image decreases as the size of the hologram decreases. Thus, a hologram is reliable method of data storage.
3. Another characteristic which proves the supremacy of a hologram over a photograph is its information storage capacity. Superposition of several images on a photographic plate is senseless. (Only one image can be recorded on a photographic plate). A hologram, on the other hand, may contain a number of consecutively recorded scenes that can be recorded independently. Different scenes can be recorded on a hologram by changing the angle, in each case, at which the reference wave is incident on the holographic plate. This can be done simply by rotating the plate. Reconstruction of the specific scene can be done by orienting the hologram properly with the reconstruction wave. It has been estimated that a single hologram with a area about 100 cm^2 may contain at least one volume of Encyclopaedia Britannica. This indicates the extremely high information capacity of the holograms.
4. In photography the prints on the photographic paper is produced from the negative, which is an image usually formed on a transparent plastic film. The negative is produced by exposing the film to the light from the object. In the exposed film the darkest areas correspond to the lightest areas of the object and vice versa.

   Another curious property of the wave front reconstruction process is that it does not produce negatives. One may consider hologram itself as a negative. But the image it produces is positive. We can produce the copy of the hologram by contact printing in a reversed sense that the opaque areas now become transparent and vice versa. It can be seen that the image reconstructed from this reversed copy would be identical in all respects to that produced by the original. This is because the information is recorded on the plate in the form of a modulated spatial carrier. It may be recalled that the information on the grating carrier is embodied in the fringe contrast and in the fringe spacing; neither of these is altered by the reversal of the polarity.

Applications of the principle of holography: There are a large number of applications for holography. They are used in art, data storage, security holograms for credit cards, hologram dockets for vehicle number plate, hologram tags in electrical and electronic products, holographic scanners in post offices, shipping firms, automated conveyer systems etc. Here we consider in detail only two applications in the scientific field.

1. **Study of a microscopic particle in a transient event**: Consider the problem of locating a transient event concerning a microscopic particle in a certain volume and studying it. It is very difficult to use ordinary microscopes for this purpose. Since the information about the depth can be stored in a hologram, we can make a holographic record of the complete volume in which the particle moves. That is, we can ‘freeze’ an event in a hologram. On reconstruction, we get the same waves from the object with a difference that it is now not transient. Now we can use a microscope to locate the particle size, distribution, cross-sectional geometry etc.
2. **Application of holography in interferometry**: Another important application of holography is in interferometry. In the double exposure holographic interferometry one first partially exposes an object to the photographic plate with a reference wave. Next the object is stressed and makes another exposure with the same reference wave. If the resulting hologram is illuminated by a reconstruction wave, two object waves are emerged from the hologram, one corresponding to the unstressed object and the other corresponding to the stressed object. These two object waves would interfere to produce interference fringes. Thus, on viewing through the hologram, one sees a reconstruction of the object superimposed with the fringes. The shape and the number of fringes give one the distribution of strain in the object. This technique is employed for the non-destructive testing of the objects.

   By using the above technique one can see the footprint on a carpet on which a person had walked. With naked eye one cannot see this footprint. But it can be made visible using the above-mentioned method of double exposure interferogram on the carpet after the person had walked. Since the fibres on the carpet relax slowly, if two identical holograms are taken with a reasonable time interval between them, then the movement of the carpet surface is obvious from the interferogram.

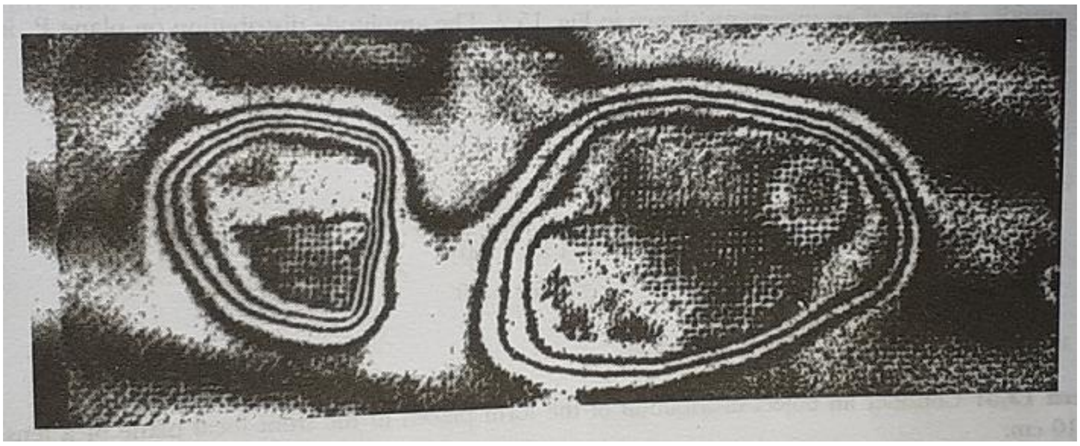

Outline of footprint on a carpet, not visible to the naked eye is revealed using holography

4.3 Industrial application of lasers

Since the laser beam has extreme directionality, extreme monochromaticity and large intensity it can be used for various industrial purposes. The beam coming out of the laser has a spread of usually a few mm in diameter. For most material processing applications, one needs large intensity and very strong electric field over a very small area. This can be achieved by focussing the laser beam over a small area by using a lens. Using the theory of diffraction by a circular aperture we can show that the radius 'b' of the circular region over which the beam is focussed by a lens of focal length 'f',

$$b = \frac{\lambda f}{a} \qquad (1)$$

where, λ is the wavelength of laser light and 'a' be the radius of the laser beam. If P is the power (energy flow per second) of the laser beam, the intensity (power per unit area) of the beam is given by,

$$I = \frac{\text{Power per unit area}}{\text{Area}} = \frac{P}{\pi b^2} = \frac{Pa^2}{\pi \lambda^2 f^2} \qquad (2)$$

Example: Find the intensity at the focussed spot of a 1 watt laser beam of wavelength 1.06 μm and having a beam radius 1 cm focussed by a lens of focal length 2 cm. Also find the radius of the beam at the focus.

Radius of the beam at the focus, $b = \frac{\lambda f}{a} = \frac{1.06\times10^{-6}\times2\times10^{-2}}{10^{-2}}$

$= 2.12\times10^{-6}$ m $= 2.12\times10^{-4}$ cm

Intensity, $I = \frac{P}{\pi b^2} = \frac{1}{3.14\times2.12^2\times10^{-12}}$

$= 7.1\times10^{10}\ \text{W/m}^2 = 7.1\times10^{6}\ \text{W/cm}^2$

Moreover, it can be shown that the electric field strengths produced at the focus are of the order of 10^7 V/cm. This shows that the intensity and field strength are very large at the focus. This finds a large number of applications in the industrial field. The following gives a number of industrial and commercial applications of laser. We study in detail only a few of them.

Lasers are used in industry in a huge variety of applications. These applications can be divided between those that involve the processing of materials and all other applications like laser tracking, Lidar, precision length management, laser interferometry, speckle metrology, velocity measurement, surveying and ranging etc. Materials processing includes cutting, drilling, welding, etc., and generally involves the use of high-powered lasers.

A detailed list of industrial and commercial laser applications includes:

- Laser cutting
- Laser welding
- Laser drilling
- Laser marking
- Laser cleaning
- Laser cladding, a surface engineering process applied to mechanical components for reconditioning, repair work or hard facing
- Photolithography
- Optical communications over optical fiber or in free space
- Laser peening

- Guidance systems (e.g., ring laser gyroscopes)
- Laser rangefinder / surveying,
- Lidar / pollution monitoring,
- Digital minilabs
- Barcode readers
- Laser engraving of printing plate
- Laser bonding of additive marking materials for decoration and identification,
- Laser pointers
- Laser mice
- Laser accelerometers
- OLED display manufacturing
- Holography
- Bubblegrams
- Optical tweezers
- Writing subtitles onto motion picture films.
- Power beaming, which is a possible solution to transfer energy to the climber of a Space elevator
- 3D laser scanners for accurate 3D measurement
- Laser line levels are used in surveying and construction. Lasers are also used for guidance for aircraft.
- Extensively in both consumer and industrial imaging equipment.
- In laser printers: gas and diode lasers play a key role in manufacturing high resolution printing plates and in image scanning equipment.
- Diode lasers are used as a light switch in industry, with a laser beam and a receiver which will switch on or off when the beam is interrupted, and because a laser can keep the light intensity over larger distances than a normal light, and is more precise than a normal light it can be used for product detection in automated production.
- Laser alignment
- Additive manufacturing
- Plastic welding
- Metrology - handheld and robotic laser systems for Aerospace, Automotive and Rail applications
- To store and retrieve data in optical discs, such as CDs and DVDs
- Blu-ray

Entertainment and recreation

- Laser lighting displays accompany many music concerts
- Laser tag
- Laser harp: a musical instrument were the strings are replaced with laser beams
- As a light source for digital cinema projectors

4.3.1 Application of laser in material processing

Industrial laser applications can be divided into two categories depending on the power of the laser: material processing and micro-material processing.

In material processing, lasers with average optical power above 1 kilowatt are used mainly for industrial materials processing applications. Beyond this power threshold there are thermal issues related to the optics that separate these lasers from their lower-power counterparts. Laser systems in the 50-300W range are used primarily for pumping, plastic welding and soldering applications. Lasers above 300W are used in brazing, thin metal welding, and sheet metal cutting applications. The required brightness (as measured in by the beam parameter product) is higher for cutting applications than for brazing and thin metal welding. High power applications, such as hardening, cladding, and deep penetrating welding, require multiple kW of optical power, and are used in a broad range of industrial processes.

Micro material processing is a category that includes all laser material processing applications under 1 kilowatt. The use of lasers in Micro Materials Processing has found broad application in the development and manufacturing of screens for smartphones, tablet computers, and LED TVs.

4.3.1.1 Laser welding

One of the simplest application of lasers is in welding. High temperature is required melt and join materials like steel. So high power lasers have found many applications in the area of welding. As an example, carbon dioxide lasers emitting a wavelength of 10.6 μm and with a power of 6 kW of power are used for welding of $\frac{1}{4}$ inch thick stainless steel. Another example is pulsed ruby laser having an energy of 5 J with pulse duration of about 5 ns was used in welding of 0.18 mm thick stainless steel. Laser welding has the following important uses.

1. In automobile industry for welding of different parts.
2. In electronics and microelectronics for precise welding.
3. For welding two dissimilar metals like thermocouple.
4. For attaching probes to transistors, turbine blades etc.

   Nd:YAG and CO_2 laser are the two important kind of lasers that find wide ranging applications in welding.

4.3.1.2 Hole drilling

Drilling of holes in various substances is another application of lasers. The advantages of laser drilling are,

1. Laser drilling has the advantage precise location of the hole.
2. Laser drilling reduces very much the drilling time. Typical drilling speeds of 1 cm/sec is possible by using different types of lasers.
3. Due to the extremely small areas to which the laser beam can be focussed, they can be used in the area of micromachining. For example, one can write on a human hair using lasers.

Following are some examples of laser drilling.

1. A laser pulse of pulse width about 0.01 s and energy 0.05 J can make a hole of radius 0.1 mm in a 1 mm thick steel plate.
2. Drilling of diamond dies used for drawing wires.
3. One can easily drill holes as small as 10 μm through the hardest of substances.
4. Swiss watch industry uses Nd:YAG laser to drill ruby stones used in timepieces.
5. Laser can be used to remove the microscopic quantities of material from balance wheels while in motion.
6. They can also be used in trimming resistors to accuracies of 0.1%. Such micro-machining process fond widespread use in semiconductor circuit processing.

4.3.1.3 Laser cutting

Lasers also find application in cutting materials. Most common laser use for this purpose is CO_2 laser due to its high output power. A cutting process is actually a drilling process. Here the frequency of the laser pulse and the motion of the laser across the material are adjusted so that a series of partially overlapping holes are produced. The width of the cut may be adjusted to very small. But it should not be very small and should have a minimum width such that no rewelding of the cut portion takes place.

In some cases, it is advantageous to use highly reactive gases like oxygen while cutting so that when the laser heats up the material burning takes place. The gas jet also helps in expelling the molten material. Such a method is used to cut stainless steel, low carbon steel, Titanium, etc.

In some methods, inactive gases like nitrogen or argon is used instead of oxygen. This gas jet helps only in expelling the molten material. This technique is very efficient with materials which absorb most radiation at the laser wavelength. Wood, paper, plastic, etc. have been cut using such a method. Laser cutting finds widespread application in the aircraft and automobile industries.

4.3.1.4 Other applications of material processing

Lasers can be used in vaporising materials for subsequent deposition on a substrate. The unique advantages of this process is that no contamination occurs, some preselected areas of the source material may be evaporated, or the evaporant may be located very close to the substrate.

One interesting application of laser is in the opening of oysters (Oyster is the common name for a number of different families of salt-water bivalve molluscs that live in marine or brackish habitats. In some species, the valves are highly calcified, and many are somewhat irregular in shape. Many, but not all oysters are in the superfamily Ostreoidea). A laser beam is focussed on that point on the shell where the muscle is attached. This results in detachment of the muscle, the opening of the shell, and leaving the raw oyster alive in the half shell.

4.3.2 Laser Tracking

By tracking we imply the determination of either the trajectory of a moving object like aircraft, rocket, etc. or the daily positions of the heavenly objects like moon, artificial satellites etc. A review of laser tracking system was given by Lehr in 1974. The basic principle of laser tracking is essentially is the same as that used in microwave radar systems.

In the laser tracking technique, a sharp laser pulse (or, modulated continuous wave laser) is sent to the object to be tracked and the reflected wave from the object is received. By measuring the time taken by the laser pulse to travel to and fro the object can be tracked. Typical lasers used for tracking includes Nd:YAG, GaAs, Ruby, Nd:Glass.

The main advantage of laser tracking system is that not only it has smaller size but also the lesser cost. Moreover, the laser radar offers much higher spatial resolution.

In many cases one can use a retroreflector on the object to be tracked. In a retroreflector the incident and the reflected rays are parallel and travel in the opposite directions. A cube corner can be used to act as a retroreflector.

Disadvantages

1. When fog and snow are present in the atmosphere, it is extremely difficult to work at optical frequencies.
2. During daytime there is a large background noise.
3. The losses in the transmitter and receiver are also considerably larger in the laser systems.

National Aeronautic and Space Administration U S A had launched an aluminium sphere called the Laser Geodynamic Satellite (LAGEOS) into the orbit surrounding the earth at an altitude of 5800 km for studying the movements in the earth's surface, which could be great help in predicting earthquakes.

4.3.3 LIDAR

Lidar is the acronym for light detection and ranging. They have been used for monitoring the environment. Laser systems can be used as lidar. In this system laser pulses are sent to the atmosphere. These pulses are scattered by various particles present in the atmosphere and the scattered radiations are received by a receiver. The background sunlight is removed by using filters. The scattered light gives the information about the particles present in the atmosphere.

In order to study the aerosols (colloidal suspension of solid particles or liquid droplets in air or other gases) present in the atmosphere a pulsed lidar system can be used. For that one usually measures the time dependence of the intensity of the backscattered laser light using a photodetector. Then this time variations can be easily converted into height variations (time of

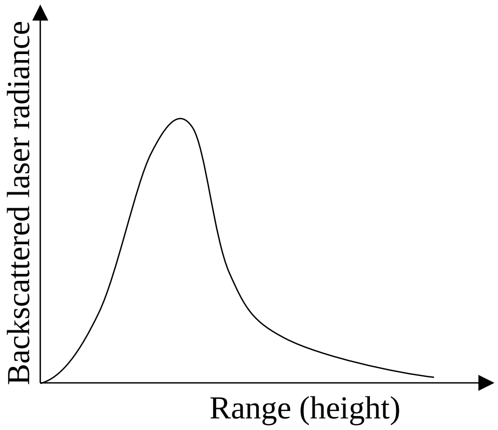

Fig.a: Backscattered radiation from clear atmosphere

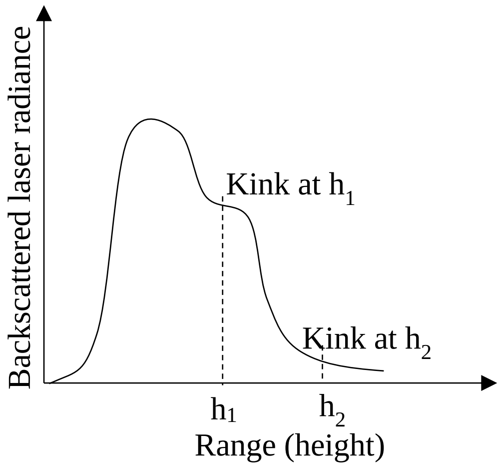

Fig.b: Backscattered radiation from atmosphere containing aerosol

travel is equal to 2h/v) from which the laser beam has been backscattered. A typical time dependence of the backscattered laser radiation by atmospheric air in the absence of aerosols is as shown in fig.a. In this case the backscattering is due to the molecules of different gases such as N_2, O_2, Ar, etc. If the aerosols are present, we get a different graph as shown in fig.b. The kinks appear in the curve at heights h_1 and h_2 are due to the fact that in between the heights h_1 and h_2 there are aerosols present in the atmosphere, which are responsible for the greater intensity of the backscattered laser light. Fig.b also shows that beyond the height h_2 one does not expect the presence of any aerosols. In addition to this lidar can also be used for other purposes given below.

1. With lidar one can also study the concentrations and sizes of the various particles present in the atmosphere, which are of extreme importance in pollution studies.
2. It is difficult to detect small particles with microwave radar. But lidar can detect particles that can scan scatter in the optical wavelengths.
3. Lidar can be used to study the visibility of the atmosphere.
4. It can be used to study the diffusion of a particulate material, or, gases released at a point in the atmosphere.
5. It can also be used study the presence of clouds, fog, etc.
6. Lidar is also used to study turbulence and winds and the probing of the stratosphere.

4.3.4 Precision length measurement

The important characteristics of laser is that it has large coherence length and its output has high intensity coupled with low divergence. These properties enable the laser to find applications in precision length measurements using interferometric techniques.

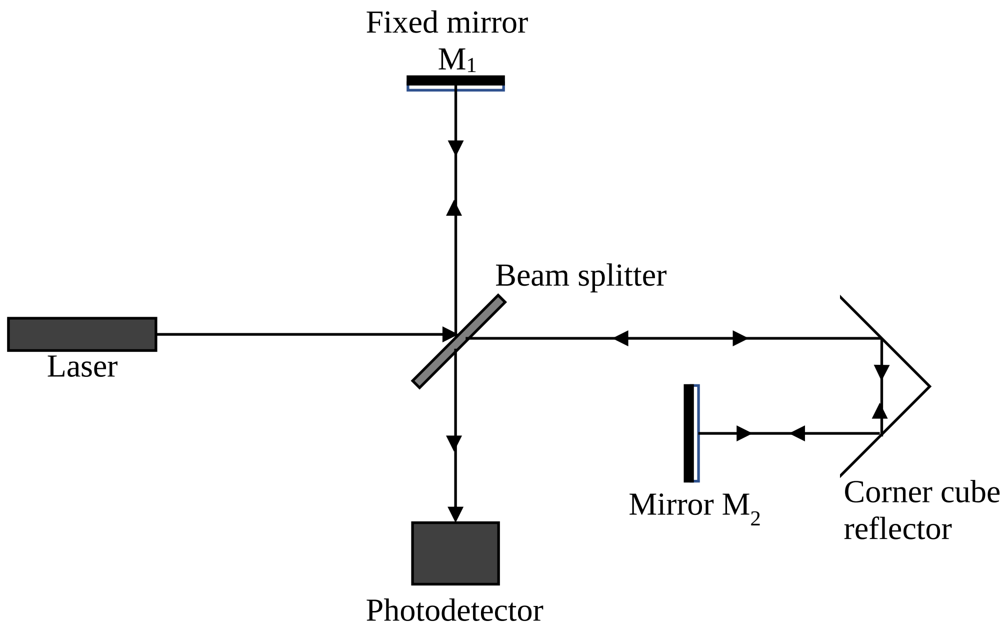

The arrangement is as shown in the figure. It consists of a beam splitter which splits the laser beam into two portions, say beam I and beam II. Beam I is reflected back by the mirror M_1 and beam II is reflected back by the retroreflector (corner cube reflector). Finally, these two reflected beams reach the photodetector. The two reflected beams reaching the detector interfere to produce either constructive interference or destructive interference. Now the reflecting surface (beam splitter) is slightly moved (translation not rotation) right (of the order of wavelength of the laser light). Then one would obtain alternatively constructive and destructive (bright and dark bands) interference, which can be detected with the help of photodetector. The distance travelled by the reflector corresponding to consecutive constructive and destructive interference is equal to half of the wavelength of the laser beam. Thus, one can measure the distance traversed by the surface on which the reflector is mounted by counting the number of fringes which have crossed the photodetector. Accuracies up to 0.1 μm can be obtained by this technique.

He-Ne laser is most commonly used for the precision length measurements. This technique is used for the following purposes.

1. For the accurate positioning of aircraft components on a machine tool.
2. For calibration and testing of machine tools
3. For comparison with the standards.
4. For many other precision measurements.

4.3.5 Laser interferometry and Speckle metrology

The field which uses interference phenomena for accurate measurements is referred to as interferometry. This technique is widely used in science, technology and engineering. An interferometer divides the light beam into two or more parts and finally united together to produce interference pattern. The laser interferometer, which uses laser beam, can be used for high precision measurements from a few nanometres to about 100 m for measuring distances, angles, flatness, straightness, velocity, acceleration, vibration etc. Accurate measurement of displacement is very crucial in many industries such as machine tool industries, integrated circuit manufacturing industries etc.

Common lasers that are used in interferometry are He-Ne laser, Argon ion laser, Nd:YAG laser and diode laser. Among these, diode lasers are most compact with low power consumption and are available over a very broad range of wavelengths. They are also tuneable over a limited wavelength range.

Depending upon the frequencies of the two interfering beams there are two types of interferometry. If the two interfering beams have same frequency and the output intensity remains constant the interferometry is referred to as *homodyne interferometry*. In contrast in *heterodyne interferometry* the laser is made to emit two closely lying frequencies.

Speckle metrology: Speckle is the shimmering effect that you've seen every time you use a laser pointer. From a technical perspective, speckle is an interference pattern that occurs when coherent light is scattered off an optically rough surface, such as a screen. Since laser beams consist of coherent light, they will usually exhibit speckle. It is observed as visible 'noise' on a uniform area of the scene and decreases the perceived contrast of the pictures; is most visible on uniform, bright scene elements. Speckle is more visible when the viewer moves their head back and forth.

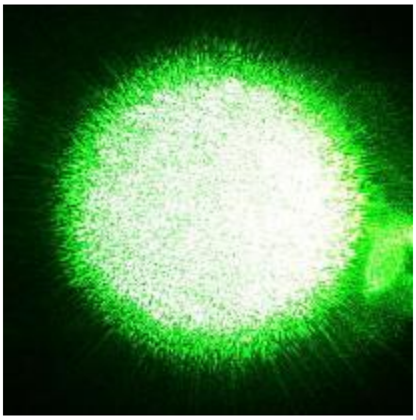

While speckle is inherent in any laser light source, researchers have developed very effective means of virtually eliminating visible speckle in state-of-the-art laser illuminated projector systems. But due to the optical characteristics of the speckle phenomenon, it is difficult to make accurate and repeatable measurements. For example, the measured results depend on type of instrumentation used, exposure time, measurement distance, screen surface characteristics and many other factors that -until now- have not been defined to assure consistent results.

The field of speckle metrology has seen a surge in development in the past 10 years owing to advancements in digital cameras and computing power. For instance, a variety of digital speckle correlation (DSC) processes can now be performed in almost real time and therefore speckle techniques has found applications in non-destructive testing (NDT), biology, and medicine. New techniques in terms of optical arrangements and in extracting phase data have been introduced for measuring out-of-plane and in-plane motions in digital speckle interferometry (DSPI) and digital speckle shear interferometry (DSSPI). DSC, DSPI, and DSSPI have also been combined to extend the range of measurements. In addition, quantitative analysis in speckle interferometry has seen a plethora of new software developments for conducting real-time, accurate, complicated, fast, and repeatable measurements with ease. In addition, different methods to process speckle fringes have made analysis equivalent to that of classical interferometry, yet can be applied to all types of real-world specimen.

4.4 Lasers in medicine

Lasers find a wide range of applications in the field of medicine. Lasers used in medicine include, in principle, any type of laser, but especially:

- CO_2 lasers, used to cut, vaporize, ablate and photo-coagulate soft tissue.
- Diode lasers
- Dye lasers
- Excimer lasers
- Fiber lasers
- Gas lasers
- Free electron lasers
- Semiconductor diode lasers

Table below shows wavelengths and power of lasers used in different medical applications.

Application	Wavelengths (nm)	Power
Photodynamic therapy (PDT)	630, 635, 652, 660-690, 753	1–15 W
Low level laser therapy	465, 630, 635, 652, 660-690	0.5–10 W
Dentistry	465, 810-980	0.5–10 W
Surgery	800-1500	0.5–10 W
Hyperthermia of tumors	940, 980, 1064	15–50 W

Examples of procedures, practices, devices, and specialties where lasers are utilized include:

- Ophthalmology (includes Lasik and laser photocoagulation)
    1. Eye surgery: Hundreds of successful eye surgery have already been performed using lasers. The surgery is painless.
    2. Laser can be used for welding detached retina of the eye.
    3. Laser can be used for the correction of the focussing defects of eye. In the method referred to as LASIK (Laser In-Situ Keratomileusis) the cornea of the eye can be crafted to adjust the curvature so that the focussing by the eye lens takes place on the retina. This method can correct eye defects requiring high lens powers.
    4. Lasers are found useful for the treatment of glaucoma.
- Angioplasty
- Cancer diagnosis
- Cancer treatment: Lasers are extensively user for the treatment of cancer. New types of surgery with ultraviolet excimer lasers and high-powered pulsed neodymium laser energy transmitted through an optical fibre is now used in the treatment of liver cancer.
- Argon ion and CO_2 lasers are common sources in the treatment of liver and lungs and for the elimination of moles and tumours on the skin tissues.
- Laser can be used to destroy the tissues of the dental structures in benign ovarian cystic teratomas.
- Dentistry: The application of lasers in dentistry enables dentists to perform a wide variety of dental procedures they otherwise might not be capable of performing. When used for surgical and dental procedures, the laser acts as a cutting instrument or a vaporizer of tissue that it comes in contact with. When the laser is used for curing a filling, it helps to strengthen the bond between the filling and the tooth. In teeth whitening procedures, the laser acts as a heat source and enhances the effect of tooth bleaching agents.
- Cosmetic dermatology such as scar revision, skin resurfacing, laser hair removal, tattoo removal
- Dermatology, to treat melanoma
- Frenectomy
- Lithotripsy
- Laser mammography
- Medical imaging
- Microscopy
- Optical coherence tomography
- Optogenetics
- Prostatectomy
- Plastic surgery, in laser liposuction, and in treatment of skin lesions (congenital and acquired) and in scar management (burns and surgical scars)
- Surgery, to cut, ablate, and cauterize tissue
- Laser radiation can be used for controlling haemorrhage.

- Therapy and stomatology
    1. Light therapy
    2. Low level laser therapy
    3. Photodynamic therapy
    4. Endovenous laser therapy

4.5 Isotope separation

Another new application of the lasers, especially the tuneable lasers, is in isotope separation, which is of immense importance for nuclear power reactors. Nuclear reactors need the isotope of uranium U^{235}, which is only 0.7% of the natural uranium. This technique of laser isotope separation (LIS) is based on the fact that different isotopes absorb light at different frequencies. A particular species (isotope) is selectively excited by means of a highly monochromatic laser, properly tuned to specific resonance, and then separated from the mixture by one of the several processes available.

In LIS one makes use of the slight differences in the energy levels of the atoms of the isotopes due to the difference in nuclear mass. This difference termed as isotope shift. Thus, light of a certain wavelength may be absorbed by one isotope, while the other isotopes of the element do not absorb it.

Fig.a shows the block diagram of a typical laser isotope separation process. The laser excites one of the isotopes (selected one) from the isotopic mixture through selective absorption and then the excited isotope is separated using one of the many techniques. In the following we discuss three main techniques of isotope separation.

Introduction of the isotopic mixture in vapour form → Laser photoexcitation (selective absorption of hν) → Extraction of selected isotope

Fig.a

4.5.1 Separation using radiation pressure

This is one of the laser isotope separation methods. The principle behind this method is the deflection of free atoms or molecules by radiation pressure. When a photon is absorbed by an atom, the momentum of the atom is increased by the photon momentum $\frac{h\nu}{c}$ and hence the atom is pushed in the direction of the incident photon (laser beam).

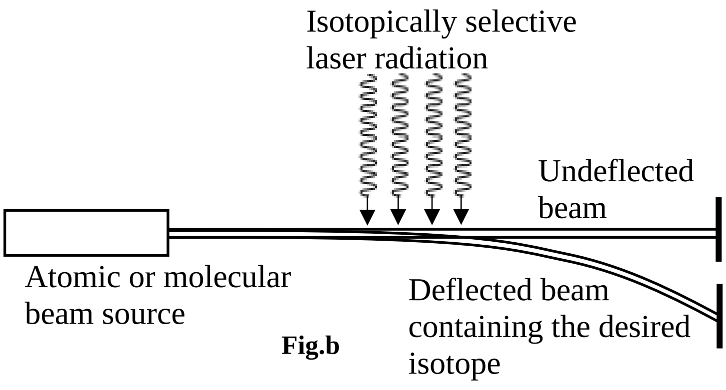

Fig.b

The momentum acquired by the atom in a single absorption is very small. To get sufficient momentum the atom must absorb many photons (not simultaneously). This requires that the atoms have a short lifetime in the excited state. This can be explained as follows. When the excited atom is dropped to the ground state, it emits a photon and acquires a momentum opposite to the emitted photon direction. Then the atom can again absorb another photon and it undergoes another emission and this process is repeated. Since the emissions occur in all random directions, the net effect of many absorptions and emissions is to push the atoms along the laser beam.

Fig.b shows the schematic diagram of the separation of the desired isotope using radiation pressure method. In this technique, the laser beam is allowed to impinge on an atomic beam at right angles. Now only the desired isotope atoms absorb the laser beam and are deflected.

Example: Separation of sodium isotope: For sodium isotopes the velocity acquired by an atom from the momentum transfer during the absorption of one photon is about 3 cm/s in the direction of laser beam. The lifetime of the atom in the excited state is 10^{-8} s. The thermal velocity of the atomic beam is 10^5 cm/s through the interaction zone (right angles to laser beam) of length 1 cm. Then,

$$\text{Time of travel in the interaction zone} = \frac{\text{Length of interaction zone}}{\text{Velocity}} = \frac{1}{10^5} = 10^{-5}\ \text{s}$$

$$\text{Number of photon absorptions} = \frac{\text{Time of travel in the interaction zone}}{\text{Lifetime}}$$

$$= \frac{10^{-5}}{10^{-8}} = 10^3$$

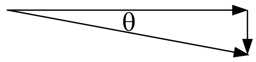

$$\text{Net gain in velocity} = \text{Gain in velocity per absorption} \times \text{Number of absorptions}$$

$$= 3\times10^3 \ \text{cm/s in the direction of the laser beam.}$$

Since the angle of deflection is small,

$$\theta \approx \tan\theta = \frac{3\times10^3}{10^5} = 3\times10^{-2}\ \text{radian} = 30\ \text{mrad}$$

This deflection is sufficient for separating the desired sodium isotope from the mixture. Such a method of separating isotopes of barium was used by Bernhardt and others in 1974.

4.5.2 Separation by selective photoionization or photodissociation

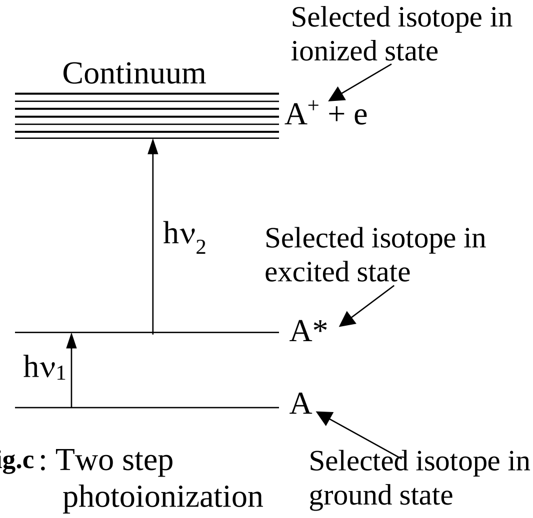

Fig.c: Two step photoionization

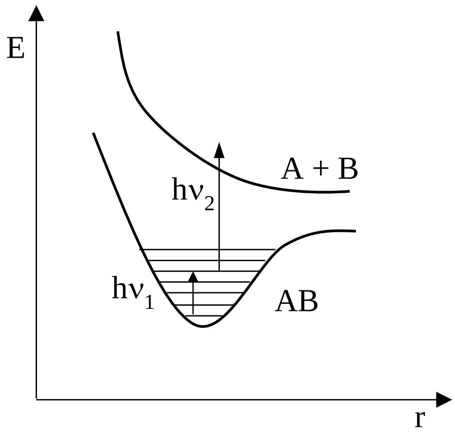

Fig.d: Two step photo-dissociation of molecule

The most popular scheme of isotope separation is the two-step photoionization of atoms (selected isotope) or the two-step photodissociation of molecules (containing the selected isotope). The first step causes the selective excitation. This is followed by a second excitation, which ionizes the excited atom or dissociates the excited molecule. In the case of atoms, the separation can be carried out by extracting the ions by means of electric field. In the case of molecules, the dissociation products are separated from the other molecules directly or by means of chemical reaction.

This two-step photoionization with laser was used to demonstrate the feasibility of LIS for uranium at the Lawrence Livermore Laboratory in U S A. Using this technique enriched uranium (60% U^{235}) was made. In this experiment the atomic beam of natural uranium (99.3%U^{238} + 0.7%U^{235}) was generated in a furnace at a temperature of 2100°C. This atomic beam is then undergone an isotopic selective excitation by dye laser and then ionized by using the light of a high-pressure mercury lamp. Then the ions of U^{235} isotope is separated.

An example of two-step photodissociation process is the separation of two boron isotopes, ^{10}B and ^{11}B, by the dissociation of BC_3 molecules (mixture of $^{10}BC_3$ and $^{11}BC_3$ molecules). In this experiment $^{11}BC_3$ molecule was selectively excited by CO_2 laser beam. The molecules excited in this manner were dissociated by using light with wavelengths between 2130 Å and 2150 Å. The fragments generated by the dissociation, originating mainly from $^{11}BC_3$ molecules were bound by reaction with O_2. It was found that with five light pulses of CO_2 laser can produce a 14% enrichment of a 5 μgm sample.

4.5.3 Photochemical separation

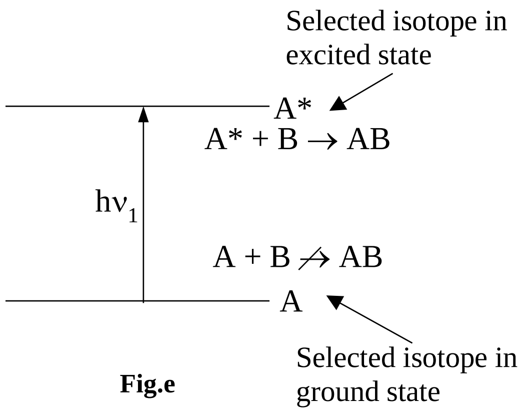

Fig.e

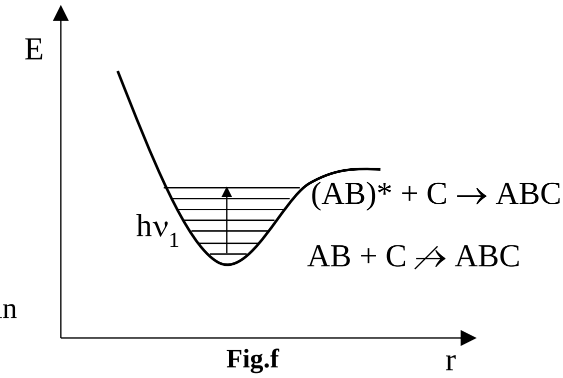

Fig.f

Another possible way of separating selectively excited atoms/molecules from those in the ground state is by means of chemical reaction. The reaction must be chosen such that it takes place only with the selected atoms/molecules in the excited state but not with those in the ground state. The isotope of interest can be separated from other isotopes by the chemical separation of the reaction products. This idea is illustrated in figures e and f.

One example is the enrichment of deuterium using HF laser. Some lines of HF laser coincide with strong transition lines of methanol (hydrogen methanol CH_3OH) but not with the corresponding lines of deuterium methanol (CD_3OD, the symbol D stands for deuterium). The excitation activates the reaction of methanol as,

$$CH_3OH + Br_2 = 2HBr + HCOOH$$

A one to one gas mixture of methanol and deuterium methanol (50% CH_3OH + 50% CD_3OD) can be converted into a mixture containing 95% CD_3OD and 5% CH_3OH by irradiating the one to one mixture with 90 watt HF laser for 60 seconds in presence of Br_2. This is because the excited methanol reacts with bromine but deuterium methanol does not.

Applications of LIS: One of the most important fields in which the laser isotope separation process finds applications in the nuclear power industry which requires uranium enriched with the isotope U^{235}. In addition to the nuclear power industry this process helps to obtain certain isotopes that are used as tracers in medicine, agriculture, research, industry etc.

4.6 Lasers in chemistry*

Using lasers one can attain high temperature and high electric fields larger than 10^9 V/cm at the focus of a laser beam. Because of the extreme high temperatures obtainable by lasers we can use it an excellent tool for triggering chemical and photochemical reactions. The electric fields produced by the laser is larger than the fields that hold the valance electrons to the atoms.

It can be demonstrated that the molecules that have been excited by an infrared laser react faster than the molecules that are in ground state. The extremely high monochromaticity of the laser allows one to selectively excite different bands of a molecule and thus leads to the possibility of producing some new chemical products.

Using intense laser pulses lasting for a few picoseconds one can study ultrafast physical and chemical processes.

With the availability of laser pulses with duration in the tens of femtoseconds, it is possible to observe in real time chemical reaction in which chemical bonds break, form or geometrically change with extreme rapidity involving motion of electrons and atomic nuclei. Today femto-chemistry finds application in studies on various types of bonds and addresses (chemistry addresses topics such as how atoms and molecules interact via chemical bonds to form new chemical, compounds) in complex molecular systems, from diatomics to proteins to DNA leading to new branch of *femtobiology*.

With a sufficiently intense laser radiation properly tuned to specific resonance, it is possible to break the molecules where we want to break them. A large number of laser induced chemical reactions are given in the next topic.

4.6.1 laser induced chemical reactions

[J. Thomas Knudtson and Edward M. Eyring, Department of Chemistry, University of Utah, Salt Lake City, Utah 841 12]

Lasers have found increasing use in chemistry as their versatility and reliability have developed. Infrared, visible, and ultraviolet lasers are now tuneable, both continuous wave (CW) and pulsed, with commercial models closely following new laboratory developments. Experiments that cannot be achieved with a conventional light source are often possible with lasers because of their much greater intensity, monochromaticity, narrow pulse widths, etc. Relatively a few chemical applications of lasers make use of the unique spatial and temporal coherence of laser light.

In recent editions of this series and elsewhere, Rentzepis and Moore have reviewed laser picosecond spectroscopy and lasers in chemistry, respectively. The topic of laser light scattering has been reviewed by Peticolas and Chu. Another use of laser light scattering in an entirely different vein (kinetic) has been reported by Riesner & Buenemann. Raman scattering, the complement of infrared absorption, has become a useful laboratory tool with laser light sources. An annual series is now devoted to a review of developments in this area. Chemical lasers are powerful and efficient sources of infrared radiation and there is strong interest in extending this technique to shorter wavelengths. The most promising laser from the chemist's point of view is the tunable dye laser; some of the recent developments include narrow pulses and tunable uv light. The possible achievement of laser action in the X-ray region of the electromagnetic spectrum continues to excite great interest. A coherent X-ray source could, for example, permit X-ray crystallographers to circumvent the phase problem. Several, though by no means all, of the more promising approaches to the development of an X-ray laser have been reviewed succinctly by Andrews. A flurry of excitement caused by a report of tentative evidence for an X-ray laser has since been dispelled. It now appears unlikely that an $\sim$1 Å wavelength X-ray laser with a practically significant beam intensity will appear on the scene in less than two or three years.

Having called attention above to survey articles covering a very much broader range of laser topics, we limit ourselves hereafter to a review of recent progress in the following more restricted areas:

1. Chemical reactions induced by infrared lasers,
2. Reactions induced by single ultraviolet or visible laser photons,
3. Selective two-step (STS) reactions requiring two photons for their induction,
4. Kinetic studies effected by the laser temperature jump relaxation technique.

4.6.1.1 Infrared Laser-induced Chemical Reactions

This heading refers to reactions of molecules with excited vibrations produced by absorption of an infrared laser pulse. Powerful (and increasingly tunable) infrared lasers are readily available which can excite a large (approaching 50%) number of the ground vibrational state population to the first excited level. This presents an opportunity to study reactions of molecules with a specifically excited vibration.

A unique situation exists in a gas of molecules following absorption of an infrared laser pulse: the population distribution in vibrational energy levels is extremely non-Boltzmann. Since this is not an equilibrium situation, temperature is undefined. An observer would now like to measure the reaction rate of these excited molecules with an added reagent. Unfortunately, the energy placed in a specific vibrational mode by the laser is rapidly transferred to other vibrational modes and other degrees of freedom (rotational and translational). On the fastest time scale, 1 to 1000 gas collisions, vibration-to-vibration (V-V) energy transfer takes place. Vibrational energy may be accumulated in a molecule by V-V processes,

$$A(v = 1) + A(v = 1) \rightarrow A(v = 2) + A(v = 0)$$

producing highly excited vibrational species in the time required for only a few collisions. It may also be transferred to other vibrational modes in a similarly short time. On a slower time scale, the vibrational energy is converted into rotational and translational energy by vibration-to-translation/rotation(V-T/R) processes. The effect of this relaxation is to raise the translational temperature of the gas. Finally, the temperature of the gas returns to the temperature of the cell walls by energy transport processes (diffusion and thermal conductivity). Ideally, one would prefer to study the reactions of molecules in a specific excited vibrational energy level. Obviously both V-V and V-T/R processes interfere with this ideal by spreading the vibrational energy to other levels and degrees of freedom. A difficult problem with an infrared laser-induced chemical reaction is the separation of the thermal reaction from the reaction of the vibration ally excited species. If the laser is pulsed, there is an increase in the temperature of gas following the V-T/R processes which may result in an increase in reaction rate (thermal effect). If the laser is continuous the temperature increase may reach hundreds of degrees-essentially a laser simulating a Bunsen burner. The separation of reaction rates due to higher temperatures and vibrationally excited molecules is an important and often ignored part of an infrared laser-induced chemical reaction. Early signs of the importance of vibrational energy in chemical reactions were detected by Bauer and co-workers (21) in shock tube experiments. The rate of the metathesis (double decomposition) reaction

$$H_2 + D_2 \rightleftarrows 2HD$$

measured in a shock tube could be explained by assuming the reactants had to attain a minimal vibrational excitation. Bauer et al have continued to study the same metathesis reaction using a stimulated Raman laser (ruby) to produce vibration ally excited H_2 (v = 1) and D_2 (v = 1). Their experimental results- are compared to a computer model system in which higher vibrational levels are populated by collisions on a time scale that is short compared to the V-T/R time.

Vibrational levels as high as v = 9 have significant population increases following excitation of 1 % of the molecules to v = 1 by the laser. The reaction between H_2 and D_2

$$H_2\left(v = v_c\right) + D_2 \rightleftarrows 2HD$$

is assumed to take place at a critical vibrational level v_c. However, a reaction that takes place through the atoms,

$$H_2\left(v = 5\right) + H_2\left(v = 5\right) \rightarrow H_2\left(v = 0\right) + H_2\left(v = 15\right) \rightarrow 2H$$

$$H + \frac{1}{2}D_2 \rightarrow HD$$

was not ruled out. (The non-additivity of the vibrational quantum number is a consequence of the anharmonicity of the oscillator).

The complicating effects of collisional V-V and V-R/T energy transfer can be avoided by using a molecular beam apparatus. Odiorne, Brooks & Kasper, using crossed beams of K and HCl, measured the reaction rate,

$$HCl\left(v = 0,1\right) + K \rightarrow KCl + H$$

for both HC*l* (v = 0) and HC*l* (v = 1). A pulsed HC*l* chemical laser was used to excite HC*I* molecules to v = 1 in the beam. HCI (v = 1) was found to react approximately 100 times more rapidly than HCl (v = 0). The reaction rate was found to increase only 5 times for an equivalent (8.3 kcal/mole) increase in translational energy.

Gordon & Lim have very recently reported a significant increase in the rate of the bimolecular reaction

$$NO + O_3 \rightarrow NO_2\left({}^2B_1\right) + O_2$$

following vibrational excitation of O_3 to O_3 (001) (antisymmetric stretch) by a Q-switched CO_2 laser. The reactant gases were irradiated in a fast flow reactor, and the visible emission from excited $NO_2\left({}^2B_1\right)$ was used to monitor the reaction rate. Following absorption of the laser pulse, the reaction rate increased but on the slower time scale than the laser pulse width (full width at half height, fwhh = 0.7 µsec). Subsequently, the reaction rate returned to the pre laser value on a still slower time scale (~180 µsec). To explain the observed risetime the authors postulate an intermediate step

$$O_3\left(001\right) + M \rightarrow O_3\left(010\right) \quad ; \quad M\Delta E = 338\ cm^{-1}$$

transferring the vibrational excitation to the bending mode (010) of O_3. This intermediate step model is supported by the measured rate data. The conclusion that the bending mode of O_3 is much more effective than the antisymmetric stretch in promoting the reaction is perhaps the most exciting result of laser-induced chemical reaction reported to date.

In a similar experiment Arnoldi & Wolfrum have observed a very large rate increase in reactions of HC*l* with hydrogen and oxygen atoms due to vibrational excitation. They monitored the rate of decay of infrared fluorescence from HC*l* (v = 1) following excitation with an HC*l* laser pulse. In the presence of O atoms HC*l* (v = 1) is deactivated by two processes, one a chemical reaction and the other a vibrational deactivation (V -T)

$$O + HCl\left(v = 1\right) \rightarrow OH + Cl \rightarrow HCl\left(v = 0\right) + O$$

The observed O atom concentration decreased at a rate twice that of the HC*l* (v = 1) deactivation due to the consumption of O atoms by OH

$$O + OH \rightarrow O_2 + H$$

Therefore, the measured rate of HC*l* (v = 1) fluorescence decay results exclusively from the chemical reaction and not the V-T vibrational energy deactivation. The rate of atom reaction is 10^4 greater for HC*l* (v = 1) than for HC*l* (v = 0)!. Similar enhancement of the H atom reaction with HC*l* was observed, but the separation of the two processes was not as clear.

The excitation of the second overtone or HC*l* (v = 3) reported by Ambartsum ian et al is relevant for STS (selective two-step) experiments and reactions of vibrationally excited molecules. In order to overcome the very weak absorption coefficient (1.2×10^{-3} cm^{-1} at 20 torr), a high-power Q-switched Nd glass laser and amplifier were used. The stimulated Raman effect in pyridine shifted the laser frequency from 9400 cm^{-1} to 8400 cm^{-1} and an intracavity grating used to fine tune the laser frequency through the $H\,^{35}Cl$ and $H\,^{37}Cl$, v = 0 $\rightarrow$ 3 transitions. By observing the infrared fluorescence as the laser frequency was scanned, they were able to detect the v = 0 $\rightarrow$ 3 absorption. Experiments attempting to detect reactions of HC*l* (v = 3) may be difficult as only about one in 10,000 HC*l* molecules is excited under the most optimum conditions. The lifetime of HC*l* (v = 3) at 20 torr was measured to be 16 µsec. Chang & Wolga have briefly reported in a meeting abstract the vibrationally assisted reaction

$$HF(v=3) + D_2 \rightarrow HD + DF$$

using an HF chemical laser.

Dissociation of N_2F_4 by pulsed CO_2 laser

$$N_2F_4 + \hbar\omega \rightarrow 2NF_2$$

reported by Lyman & Jensen, was attributed to a nonequilibrium, high vibrational temperature following absorption of the laser pulse. They compare the time dependence of NF_2 formation from absorption measurements with computer-generated data. The measured rate of dissociation was found to be more rapid than expected if the dissociation were caused only by the thermal effects of absorbed laser energy. The energy introduced by absorption of the laser pulse was quite large, 22 mJ/cm^3 at 22.5 torr of N_2F_4.

The same authors have also reported laser-initiated explosions of N_2F_4 and SF_6 with H_2 using a CO_2 laser pulse of several hundred millijoules. A chain reaction mechanism is proposed based on dissociation of N_2F_4 into fluorine atoms. The dissociation is proposed to be greatly accelerated by laser excitation of vibrational modes of the reactants.

The nonlinear dissociation and ionization of hydrogen molecules have been studied by Agostini et al at 10^{-4} torr pressure. The number of H^+ ions and H_2^+ ions increases with the 11th and 13th power, respectively, of focused Nd laser intensity.

Eisenthal, Peticolas & Rieckhoff have observed an anomalous luminescence from compounds containing a phenyl-phenyl or benzyl-benzyl single bond using an unfocused ruby laser. They suggest that the luminescence is from molecular fragments produced by multi photon vibrational excitation leading to dissociation. The single bond connecting the two large cyclic groups is probably very anharmonic. Because anharmonicity results in mixing of vibrational wavefunctions, multilevel vibrational excitation may be important in these molecules.

A number of experiments have been reported as laser-induced chemical reactions without the necessary consideration for thermal effects. In these cases, a few conclusions can be drawn and they are mentioned for bibliographic completeness.

Isenor & Richardson have observed the luminescence prior to and during breakdown in CCl_2F_2, SiF_4, and NH_3 gases caused by a focused, pulsed transverse excitation atmospheric (TEA) CO_2 laser. At laser intensity levels below those required to produce a spark, the luminescence originated from molecular dissociation products such as C_2 and NH_2. The spark spectrum was dominated by atomic lines. Streak photographs of the luminescence were also taken.

A pulsed CO_2 laser (30 msec pulse width) was used to initiate an explosion in a mixture of BCl_3 and H_2. BCl_3 strongly absorbs the laser radiation, producing Cl atoms, probably due to thermal processes. Motion pictures looking into the laser beam show a visibly glowing cylindrical shell propagating radially to the cell wall. A much shorter pulse width (150 nsec) was focused into a low-pressure sample of BCl_3. The rise time of the visible luminescence was much faster than the time between collisions in the gas sample. Therefore, rapid collisional V-V energy transfer cannot be the source of the visible luminescence. Absorption line broadening due to the very high electric field of the laser may allow direct laser population of the upper vibrational levels.

Experiments using continuous infrared lasers generate very high temperatures in the cylinder of gas irradiated by the laser beam. Removal of the energy deposited by absorption of the laser energy is by thermal conductivity and mass diffusion. Generally, these pressure-dependent processes are slow and there is an accumulation of energy in the gas. The temperature in the beam centre will increase until the gradient between the beam centre and the cell walls is sufficient so that energy transport by thermal conductivity is equal to the energy deposited by the laser. Some of the experiments with continuous lasers suggest that reactions taking place in the laser beam differ from thermal or Bunsen burner reactions.

Mayer et al used a continuous HF laser to selectively initiate a reaction between Br_2 and CH_3OH. Equal amounts of deuterated methanol, CD_3OD, and CH_3OH were in the reaction mixture but the CD_3OD remained unreacted. Product determination was by infrared absorption. Presumably, only CH_3OH reacted with the bromine because it absorbed the 100 W 2.6 μ laser radiation and the CD_3OD did not. Moore has concluded that this reaction was thermal in origin. The selective reaction of the CH_3OH remains unexplained.

Bauer et al have examined the CW irradiation of NH_3 by a CO_2 laser. Typically, 29 W of incident power produced a 1500°C temperature increase estimated by the light emitted from NH_2. Extensive experiments led to the conclusion that the effects are thermal. That is, the vibrational and translational degrees of freedom are in or near equilibrium with one another.

A number of cautions and criteria have been suggested for infrared laser induced reactions:

1. The temperature rise following the V-T/R relaxation should be calculated to insure that it is small. CW experiments may require use of a hot wire to simulate the energy input to the gas and an experimental measurement of the temperature. Addition of a rare gas may be used to increase the heat capacity of the gas.
2. Care must be taken to prevent reactions occurring at gas-solid interfaces. Laser heating of cell windows, dust particles, and cell walls may produce a large change in the hetero reaction rate.
3. Visible uv emissions from the laser cavity (flash lamps or plasmas) and radiation from pulsed laser power supplies may induce reactions and should be specifically excluded.
4. The reaction yield should scale with the energy absorbed.

Basov et al have irradiated a large number of gas mixtures with a continuous CO_2 laser and reported the products. The laser-absorbing gases were N_2F_4, SF_6, and BCl_3. The products and their yields were appreciably different from thermal reactions.

Yogev et al irradiated limonene and isoprene with a continuous CO_2 laser for long time periods (~1 hr). The product yields peaked at about 1 torr and after 30 torr resumed a monotonic increase. The authors claim the pressure dependence in the low-pressure region is indicative of a non-thermal reaction. The mathematical model used does not include diffusion of vibration ally excited molecules to the cell wall which plays an important part in energy transport at low pressures. Using a focused TEA CO_2 laser, Yogev et al have reported the decomposition products of cis- and trans-2-butene below the threshold for dielectric breakdown. With low pressures of 1:1 mixture they observed a net trans to cis conversion.

The effects of continuous CO_2 laser radiation on NH_3, C_2H_5Cl, C_2H_4, and BCl_3 have been reported. A pulsed Nd laser produced decomposition products in C_2H_2 and C_2D_2 mixtures.

Theory: A number of theoretical approaches to infrared laser-induced chemical reactions have been published. Generally, they involve the coupling of a master equation, describing the population of the excited vibrational levels, with a unimolecular dissociation theory.

Thermal excitation of vibrational levels is the basis of unimolecular reactions rate theory. Even those molecules that have sufficient vibrational excitation to overcome the bond energy must wait until the random phases of the excited modes finally constructively interfere and dissociation takes place. Goodman et al have theoretically calculated the effects of infrared laser excitation using both classical and quantum mechanical techniques. The former method leads to calculations of the ratio of laser-induced to thermal reactions for a variety of conditions. Rate enhancement due to laser excitation by factors up to 10^5 are calculated. However, Goodman points out that clear separation of laser induced and thermal reactions is necessary and usually difficult, particularly for pulsed or Q-switch lasers. The quantum mechanical calculations suggest a new technique for separation of the thermal and laser-induced rates. Observation of the scattered laser light at different incident laser field intensities would permit separation of the two rates.

Goodman and co-workers have recently extended their theoretical approach to include an N energy level absorber and the effects of pressure, temperature, collisional energy transfer, and stepwise absorption. The calculated rate of laser-induced reaction goes through a maximum with increasing pressure, assuming that either three or eight vibrational energy levels are pumped by the laser in an eight-level system. Absorption of laser energy by higher level transition (e.g. $v = 6 \rightarrow 7$) is very effective in rate enhancement. Experimentally very small or undetectable hot band absorption may cause observable rate increases. Coherent effects are considered and one effect may be enhanced reaction rates by multiphoton absorption. Afanas'ev et al have considered the problem of molecular dissociation following absorption of an infrared laser pulse. Only a $v = 0 \rightarrow 1$ transition is excited by the laser, and the oscillator is taken as harmonic for v-v collisional energy transfer. The energy distribution among the vibrational levels is derived from an energy diffusion approximation. With laser power sufficient to saturate the absorbing transition, sample calculations show dissociation takes place before V-T/R energy transfer.

Artamonova et al (50) combine a master equation describing the vibrational population with the Arrhenius equation for an exchange reaction

$$AB + C \rightarrow A + BC$$

A vibrational mode in AB can reach very high vibrational temperatures by v-v collisional energy transfer processes following a laser pulse. The population of the laser excited mode is described by a Boltzmann distribution with a temperature much higher than the other vibrational, rotational, and translational degrees of freedom. This temperature is used in the Arrhenius equation to describe the expected rate of reaction. The relative increase in bimolecular reaction rate constants due to vibrational excitation has been derived by Morrey in a manner similar to that of absolute reaction rate theory. Large increases in overall reaction rate result from reactant excitation.

Gordiets, Osipov & Shelepin consider the unimolecular dissociation of vibrationally hot molecules by solving the simultaneous equations describing the vibrational population below the dissociative level. Using an anharmonic Morse potential to describe the excited oscillator, they find that the extra internal energy of non-equilibrated molecules increases dissociation and permits reaction paths that are energetically unfeasible with equilibrated molecules. They suggest the hydrogen-chlorine chain reaction may be enhanced by a branching reaction of vibrationally hot HCI.

$$HCl^* + Cl_2 \rightarrow HCl + Cl + Cl$$

The probability of infrared multiphoton dissociation of a heteronuclear diatomic molecule has been calculated by Pert. The molecule is taken to be nearly harmonic. Approximate calculations for the dissociation threshold of SiF_4 are in reasonable agreement with experimental results using a CO_2 laser.

The collisional V-V energy transfer processes which populate highly excited vibrational levels are generally insensitive to different isotopic species. If a single isotope is excited, V-V energy transfer will rapidly excite the other isotopic species. Belenov et al, however, have calculated that isotope separation can take place in such systems. The energy level differences between isotopes increase as the square of the vibrational quantum number. Belenov et al show that the reaction rates are sensitive to the different vibrational frequencies of the isotopes for reactions taking place from energy levels with large quantum numbers (large activation energy).

Smith & Wood have calculated rate constants for the reactions $H + H_2$ (v = 1 and 2), $H + ClH \ (v = 1 \text{ and } 2)$, and $Cl + HCl$ (v = 1 and 2). They find that vibrational excitation lowers the activation energy for all reaction values. Because the products have a wide distribution of vibrational energies, these reactions, which may not be synthetically useful, are important paths for vibrational deactivation.

4.6.1.2 Ultraviolet visible laser-induced chemical reactions

Isotope Separations: The monochromaticity, high intensity, and in some cases tunability of lasers may be particularly useful in separating a mixture of molecules differing only in the isotopes of a nucleus. There have been several attempts made to separate isotopes using a single photon to induce a photochemical reaction of only one species in a mixture. These selective single step reactions primarily use photodissociation to initiate the chemical reaction. The enrichment of uranium isotopes by lasers has recently been announced by Exxon Nuclear Company. It has been noted, however, that the cost of isotope enrichment is only a few percent of the kilowatt-hour price of nuclear reactor-produced electric power. Therefore, very efficient laser isotope separation of uranium will have only a small effect on the cost of electric power.

Ideally, to photochemically separate nuclear isotopes, one would excite a mixture at a wavelength where one isotopic species absorbed strongly and the others were transparent. Following absorption, the excited molecule or atom dissociates or ionizes and the fragments quickly react with some other reactant (scavenger) in the gas mixture. The products from this laser-induced chemical reaction could then be separated from the mixture by physical means such as distillation or chromatography. The application of lasers to isotope separation has been recently reviewed by Moore & Zittel and Letokhov. They describe the requirements for an isotopic separation as:

(a) nonoverlapping absorption spectra of the isotopes,
(b) a laser sufficiently tunable and monochromatic to excite only one isotope,
(c) a chemical reagent that will rapidly react with the excited isotope or molecular fragments following photodissociation, and
(d) conservation of selectivity throughout excitation and reaction.

Nonoverlapping absorptions are most likely to be found in the gas phase or in a solid matrix but probably not in the liquid phase. Tunable, narrow bandwidth lasers exist in the infrared, visible, and uv regions. Reactions of the excited isotopic species or its fragments will require more imaginative experimental schemes and may present the most difficult problems.

Once the excited states or photofragments have been produced they must react sufficiently fast to prevent energy transfer to the other isotopes and subsequent loss of selectivity. This is true because energy transfer between isotopic species is always resonant or near-resonant and therefore very fast, requiring in general only a few collisions for total randomization.

Tiffany, Moos & Schawlow have reported a detailed attempt to separate the isotopes of bromine $^{79\text{-}79}Br_2$ (79-79 stands for both the atoms have mass number 79) and $^{81\text{-}81}Br_2$ using a pulsed ruby laser. Their high-resolution spectra of Br_2 at 14,400 cm^{-1} showed absorption peaks assignable to each isotope. The vibrational levels of the $^3\pi_{1w}$ state reached by absorption of the ruby laser are 500 cm^{-1} to 800 cm^{-1} below the limit for dissociation into two ground state $^2P_{3/2}$ bromine atoms (kT = 210 cm^{-1} at room temperature). Ideally, specific excitation of a Br_2 isotope would lead to enhanced bimolecular addition of the excited Br_2 across the double bond in a fluorinated olefin.

A laser-induced bromination of the olefins was observed but the products were isotopically scrambled. That is, regardless of which isotope of Br_2 was excited, both ^{79}Br and ^{81}Br appeared in the brominated olefin. A careful analysis shows the reaction probably proceeds through dissociation of $Br_2\left({}^3\pi_{1w}\right)$ by collisions (~100) followed by addition of a radical bromine atom across the olefinic double bond

$$Br_2 \xrightarrow{h\nu} Br_2\left({}^3\pi_{1w}\right) \qquad 1$$

$$Br_2\left({}^3\pi_{1w}\right) + M \longrightarrow 2Br + M \qquad 2$$

$$Br + X \longrightarrow BrX \qquad 3$$

$$BrX + Br_2 \longrightarrow XBr_2 + Br \qquad 4$$

where, X is the olefin and M is any collision partner. The significant and unforeseen difficulty was that bromine atoms, not excited bromine molecules, were reacting with the olefin.

The quantum yield was found to be approximately unity for the laser-induced reaction, indicating the chain propagating reaction (step 4) was not a source of isotope scrambling. The primary source of scrambling appears to be the very rapid reaction of bromine atoms formed by collisional dissociation of the $^3\pi_{1w}$ state with ground state isotopically random bromine molecules

$$Br^{(i)} + Br_2 \rightarrow Br^{(i)}Br + Br \qquad 5$$

where, (i) indicates the selected isotope. Although they did not succeed in achieving an isotopic separation, the careful work of Tiffany et al shows resolvable isotopic lines and that laser technology can create the isotope-specific excited state.

The successful separation of hydrogen and deuterium has been reported by Yeung & Moore using a laser-induced predissociation technique. A frequency-doubled ruby laser (3472Å) was used to excite a 1: 1 mixture of H_2CO and D_2CO at 3 torr pressure. The excited state produced is known to pre-dissociate into both molecular products, H_2 + CO, and radical products, H + HCO. The free radical products, which would cause isotopic scrambling, were discriminated against by exciting to an excited electronic state of low vibrational energy. The ratio of products formed following laser excitation was H_2 : HD : D_2 : CO = 0.5 : 0.2 : 3.3 : 3.9. The D_2/H_2 ratio of 6/1 was in agreement with the relative absorption coefficients of D_2CO/H_2CO = 5 at the laser wavelength. The success of the experiment is attributable to the stability of the products of photodissociation: no fast scavenging reaction was necessary. The pre-dissociative state of D_2CO falls apart in a time shorter than the time between collisions, therefore eliminating the problem of energy transfer to H_2CO. Although the economics of this hydrogen-deuterium separation are not yet proven, the added separation of the carbon isotopes by the method proposed by Yeung & Moore may be commercially important.

Letokhov has considered a model system for separation of two molecular isotopes using a laser to excite them to a pre-dissociative state. When the two molecules have equal probabilities of pre-dissociation and relaxation, separation will result only when one absorbs the laser light more strongly than the other. The time required for dissociation should be much less than the time required for energy transfer. However, if the lifetime of the pre-dissociative state becomes too short, line broadening will result in lessening the probability of selective excitation. These restrictions limit the excited state dissociation rate, w, to 10^7 sec^{-1} < w < 10^{10} sec^{-1}.

The low dissociation energies of I_2 and Br_2 and their well-known visible absorption spectra may be particularly suitable for a laser-induced isotope separation. The spectra of bromine isotopes have been resolved using a single mode 5145 Å argon ion laser. Within the laser linewidth, Dworetsky & Hozack were able to selectively excite transition in $^{79\text{-}79}Br_2$, $^{79\text{-}81}Br_2$ and $^{81\text{-}81}Br_2$. Similarly, I_2 has been studied using argon ion and He-Ne lasers, and the photochemistry of I_2 has been carefully reported by Sullivan. The $H_2 + I_2$ reaction goes through iodine atoms, which might present problems of isotopic scrambling by reaction (5) observed by Tiffany.

Tomlinson et al have used a continuous wave cadmium laser (λ = 325 nm) to photo-induce crosslinking in polymethylmethacrylate. The resulting increase in refractive index in the laser-illuminated areas (due to increased density) may be useful in making diffraction gratings and three-dimensional dielectric holograms.

Multiphoton Reactions: The probability of absorbing two photons simultaneously increases with the square of the laser power density. The high peak power densities from focused Q-switched and mode-locked lasers may result in two or more photon absorptions leading to a photochemical reaction. Multiphoton absorption is generally an inefficient process requiring a focused laser pulse and is limited by dielectric breakdown (spark) at high powers.

Pao & Rentzepis have initiated the polymerization of styrene, paraisopropylstyrene, and chlorine substituted derivatives of styrene with a focused ruby laser. The monomer is transparent at the fundamental laser frequency (6943 Å).

Speiser & Kimel have studied the two-photon photolysis of CHI_3 in different organic solvents (hexane, substituted benzenes, toluene, etc). Different quantum yields were attributable to different self-focusing properties of the solvent. The authors propose to use the laser-induced chemical reaction to determine the degree of self-focusing in a solvent. They have also considered higher order effects in (multiphoton) chemical reactions.

Azomethane ($C_2H_5NNC_2H_5$) has been photo-decomposed into nitrogen and hydrocarbons by a two-photon process. The quantity of N_2 produced varied as the square of the ruby laser intensity.

Verdieck has reported the production of acetylene, methane, ethylene, methylacetylene, allene, and buta-l,3-diyne from direct heating of carbon targets with a ruby laser. CCl_4, SiH_4, and GeH_4 were also produced with appropriate targets. Both Verdieck and Porter have reported initiation of the $Cl_2 + H_2$ chain reaction with a ruby laser. Porter has demonstrated that the initial step is photodissociation of Cl_2 by two-photon absorption. Cl_2 is transparent at 6943 Å but has its first absorption maximum at 3476 Å which is known to lead to dissociation. The reaction does not take place with a conventional pulse because of the higher power required for two photon absorption.

Epstein & Sun have reported the products from a focused ruby laser spark in CH_4, CH_4-N_2, CO_2-D_2, H_2-N_2, O_2-N_2, and graphite-H_2. The pattern of product formation represents high temperature reactions rather than reactions from ionizing radiation. Matheson & Lee generated $_1\Delta$ oxygen with a continuous wave Nd-YAG laser and measured its rate of reaction with five chemical acceptors such as 9,10-diphenylanthracene and rubrene. Three photon ionization of potassium vapor has been observed by Agostini & Bensoussan using a pulsed dye laser. The effects of linearly and circularly polarized light on the ionization process were studied.

A unique method using laser radiation to selectively deflect atomic isotopes in a molecular beam has been proposed by Ashkin. The resonant radiation pressure force on a neutral atom would be used to select and deflect a single isotopic species from a molecular beam. An estimated collection rate of 10^8 atoms/sec for ^{23}Na is probably too slow for preparative purposes. In an abstract, Gelbachs & Hartwick indicate partial pressure differences of ~1 % due to absorption of a few watts of infrared or visible laser power. They suggest that isotope enrichment of 100% is possible for small partial pressure differences.

4.6.1.3 Selective two step laser-induced chemical reactions

Selective two step (STS) laser-induced chemical reactions use two photons of different energy, one infrared and the other uv visible, to selectively excite a specific molecular or atomic species in a mixture. Figure 1 below shows the two-step process. The lower energy photon $\hbar\omega_1$ excites a vibrational transition, not necessarily the $v = 0 \rightarrow 1$ transition, of the specific isotope that is to be selectively excited. Impinging on the sample simultaneously is the second photon with greater energy $\hbar\omega_2$. This photon excites the molecule to a state leading to dissociation or ionization. The fragments or ions may then react with an added reagent. It is important that the molecule be transparent to the high energy photon, $\hbar\omega_2$, in the absence of the infrared photon, $\hbar\omega_1$. In essence, the infrared photon is selectively populating a hot band in the visible u-v spectrum. For good selectivity the thermal population of the infrared level should be small, $\hbar\omega_1 >> kT$. If this were not the case, the $\hbar\omega_2$ radiation would excite thermally populated hot bands.

The two-step method is intended to increase the selectivity of the excitation for separation of molecules differing in isotopic nuclei. In general, isotope shifts are well resolved in the infrared, whereas in the uv visible region the shifts are small and often overlapping. The shift of a molecular vibrational frequency due to a heavier or lighter isotopic nucleus increases with increasing vibrational quantum number. This effect can be used to provide greater resolution of vibrational lines by exciting the overtone, $v = 0 \rightarrow 2$, or second overtone, $v = 0 \rightarrow 3$. The probability of absorption, however, falls off dramatically for these forbidden transitions.

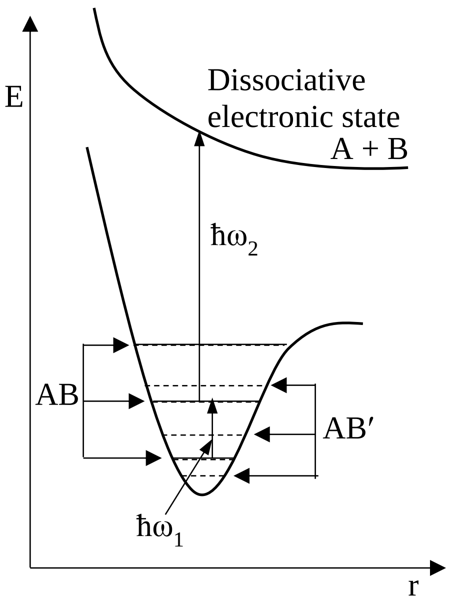

Fig.1 : Selective two-step excitation process

Ambartzumian & Letokhov have examined the requirements of possible STS reactions and described two STS reactions they have studied experimentally. A ruby laser pumped, tunable dye laser was used to excite a visible transition in Rb, which subsequently absorbed a uv photon causing ionization. The uv light was generated by frequency doubling part of the ruby laser pulse and ionization was detected with two electrodes in the cell. Only when both visible and uv laser pulses were present was a signal detected.

The second two step reaction was developed around HC*l* using infrared and ultraviolet wavelengths. The HC*l* second overtone, $v = 0 \rightarrow 3$, was excited with a Raman shifted 1.06 µm Nd laser pulse, which could be tuned to either the $H^{35}Cl$ or $H\,^{37}Cl$ absorption line. A second uv photon was obtained by frequency quadrupling a portion of the 1.06 µm laser pulse. Following photodissociation the C*l* atom would react with NO. No product yields were reported. Loss of selectivity due to vibrational energy transfer is not significant if the uv laser pulse width is less than the time required for energy transfer.

A drawback of this STS method is the high laser power required for the ionizing or dissociating radiation. Cross sections for photodissociation are 10^{-7} to 10^{-10} smaller than cross sections for absorption. Therefore, in order to photo-ionize or dissociate every molecule specifically excited by an infrared laser pulse, one needs a uv laser 10^7 to 10^{10} times more powerful. The present lack of high power uv lasers may well be overcome in the near future.

An STS reaction designed to separate $^{14}NH_3$ and $^{15}NH_3$ has been reported by Ambartsumian et al. A pulsed CO_2 laser operating on the P(32) line of the 10.6 µm branch was used to excite a $v = 0 \rightarrow 1$ vibrational transition in NH_3. The uv absorption was monitored simultaneously in the 2200 Å region with a CW uv lamp. The authors were able to detect changes in the uv absorption due to the increased population of NH3 (v = 1) vibrational level. The time dependence of the uv absorption followed the CO_2 laser pulse shape (~ 2 µsec wide) but did not return immediately to the baseline. The long tail of the transient uv absorption was due to the increase in temperature of the gas following vibrational-to-translational relaxation and subsequent higher population of the upper vibrational level. The authors estimate that 45% of the NH_3 molecules were excited to the v = 1 level following absorption of the 50 mJ laser pulse.

Recently the same authors have reported the successful separation of ^{14}N and ^{15}N using a similar experiment. The uv light source ($\hbar\omega_2$) was pulsed simultaneously with the CO_2 laser ($\hbar\omega_1$) which vibration ally excited $^{15}NH_3$. The selective photolysis of $^{15}NH_3$ results in the formation of $^{15}N_2$

$$NH3 + \hbar\omega_1 + \hbar\omega_2 \rightarrow NH_2 + H$$

$$NH_2 + NH_2 \rightarrow N_2H_4$$

$$N_2H_4 + H \rightarrow N_2H_3 + H_2$$

$$2N_2H_3 \rightarrow 2NH_3 + N_2$$

Mass spectral analysis of the product mixture originally containing equal parts $^{15}NH_3$ and $^{14}NH_3$ showed that molecular nitrogen was 80% ^{15}N and 20% ^{14}N. The amount of $^{15}NH_3$ photodissociated was reported to be several percent and was determined by the uv absorption.

Letokhov has suggested that the two step process is sufficiently selective to separate nuclei differing only in their nuclear excitation. A nucleus with 0.5 meV excitation has an increased mass, $\Delta m = Ec^{-2}$, sufficient to produce an observable shift in a molecular infrared frequency. Should high concentration of excited nuclei become available, this concept could ultimately lead to extremely short wavelength lasers in the gamma ray region.

4.6.1.4 Laser temperature jump relaxation method experiments

Continuing our descending order of specificity of laser-induced chemical reactions, we finally come to a case that those interested in the field may conceivably regard as too gross to be related to the techniques described above: Q-switch lasers can function as remarkably speedy Bunsen burners that readily heat a liquid solvent more rapidly than all but the fastest solute chemical reactions can respond (" relax "). Eigen's concept of a temperature jump relaxation method of measuring rates (and deducing mechanisms) of very rapid chemical reactions near equilibrium is now twenty years old. Over most of the intervening years the method of choice for effecting such temperature jumps in liquids has been resistive (Joule) heating effected by the rapid discharge of a low inductance, high voltage capacitor through the sample liquid. The electrical resistance of the sample is usually decreased by the addition of an inert, strong electrolyte, so that in the case of aqueous solutions, a 10° temperature jump can be effected in as short a time as 50 nsec, although 2 µsec would be more typical. The detection of the consequent relaxation of a temperature-sensitive solute equilibrium to concentrations characteristic of the new higher temperature has usually been done spectrophotometrically by fast oscillographic techniques. The only significant exception to the above generalizations until fairly recently was the occasional use of microwave heating where sample solution electrical conductivity was, of necessity, very low (i.e. pure water, pure D_2O, and solutions in low dielectric constant solvents).

Almost as soon as lasers were first reported, relaxation method kineticists began speculating about and attempting laser heating temperature jump reaction rate studies. One of the more elegant of these early experiments was the conductometric detection of a 3 µsec or longer time scale relaxation of the nickel acetate complex formation equilibrium in aqueous solution using Q-switched ruby and neodymium lasers. Koffer has re-examined essentially the same experimental system and has suggested improvements in sample cell construction (to damp pressure waves) as well as a means of eliminating error in the measured relaxation time introduced by the high frequency bridge.

Fundamental problems with laser heating at visible wavelengths using a ruby (694.3 nm) or frequency doubled Nd: glass (530 nm) laser are that a dye is typically present to absorb sufficient laser light to effect a reasonable temperature jump, say 5°. This dye must be

1. chemically inert to the solvent and sample reagents,
2. transparent to wavelengths at which spectrophotometric detection of sample concentration variation is to be performed, and
3. capable of converting its electronic excitation energy to thermal energy of solution on a time scale that is short compared to the chemical relaxation of interest.

Caldin and coworkers have found several dyes that meet these criteria with a non-Q-switched ruby laser. The one reservation is that the shortest measurable chemical relaxation times of the sample equilibria in their laser temperature jump instrument are of the order of 500 µsec.

Caldin, Grant & Hasinoff used a Nd: glass laser (without Q-switching) to effect 0.3 to 0.6°C temperature jumps in aqueous solutions of nickel(II) and cobalt(ll) with ammonia or pyridine-2-azodimethylaniline as potential ligands. Their sample cell can be pressurized up to nearly 3 kbar so that they were able to report volumes of activation in addition to rate constants and the more common ΔH^{+}_{+} and ΔS^{+}_{+} values. Grant has made a similar high pressure laser temperature jump kinetic study of these same aqueous metal ions plus copper (II) and zinc(II) all complexed by glycine. In all cases positive values of ΔV^{+}_{+} from 5 to 12 $cm^3\ mol^{-1}$ are found for the formation of the complex that are consistent with Eigen's picture of a stretching of a metal ion-first coordination sphere water bond in the activated complex.

The real beauty of the above aqueous solution kinetic studies is that they provide a reference point for similar activation volume determinations in nonaqueous solvents. For example, Caldin & Grant have studied the kinetics of complex formation by cobalt(II), nickel(II), copper(II), and zinc(II) ions with the bidentate ligand pyridine-2-azo-p-dimethylaniline in pure glycerol up to pressures of 2.8 kbar. They deduce from volume of activation data as well as activation enthalpies and rate constants that loss of a solvent molecule from the first coordination sphere of these metal ions is not rate determining in glycerol, in striking contrast to the above ligand substitution studies in water. Instead, solvent structure effects seem to dominate the energies in glycerol.

Using the same laser temperature jump equipment, Crooks & Robinson have studied a surprisingly slow proton transfer along a hydrogen bond in a complex of bromophenol blue with aromatic nitrogen bases such as 2, 6-dimethylpyridine in chlorobenzene solvent.

The absorbance of liquid water at a wavelength of 1.06 µm is only 0.067 cm^{-1}. Thus, attempts to raise sample aqueous solution temperatures by more than a few tenths of a degree with pulses of 1.06 µm radiation from Nd: glass lasers have typically been frustrated. When an attempt is also made to effect the temperature jump on a submicrosecond time scale using a Q-switch Nd: glass laser, the problem is further aggravated by the occurrence of plasmas in the sample liquid at high power densities of the laser pulse. Another potential hazard is the possibility of producing two-photon effects.

Czerlinski suggested and is still pursuing the use of the 1.35 µm band of a neodymium laser to heat aqueous sample solutions. Absorption of energy by liquid water at this wavelength is significantly greater than at 1.06 µm. Czerlinski also foresees greater utility of the laser heating concept in temperature jump kinetic studies of biochemical systems if a helium-neon laser beam is used to spectrophotometrically sample the system and this beam passes through a small sample cell coaxially with a heating pulse from another, more energetic laser.

For those interested in measuring chemical relaxations on a tens of nanosecond time scale inaccessible to the Joule heating temperature jump technique, a recent experiment by Turner et al is especially interesting. They produce stimulated Raman emission from liquid nitrogen at a wavelength of 1.41 µm (using a focused, Q-switched Nd: glass laser), and this wavelength is absorbed some 150 times more than the original 1.06 µm wavelength. They can produce up to a 7° temperature jump in a submilliliter sample volume within 30 nsec. They have used this remarkable technique to investigate the kinetics of the aqueous tri-iodide equilibrium, $I_2 + I^- \rightleftarrows I_3^-$, the dimerization of proflavin, the transition between two different spin states of a ferrous ion complex in a nonaqueous (methanolic) solvent, and an interconversion between planar and octahedral forms of an aqueous nickel(II) complex.

This last study of a Ni(II) complex was in part a repeat of an earlier study of the same chemical equilibrium in which 1.06 µm laser radiation was used to excite a specific vibration of the octahedral form of the solute rather than to heat the solvent. Still an earlier case of specific vibrational excitation of a reactant by a laser was reported by Goodall & Greenhow. They succeeded in remeasuring the rate constant for the reaction $H^+ + OH^- \rightarrow H_2O$ in water by vibration ally exciting the water to induce the process $H_2O^* \rightarrow H^+ + OH^-$. The interest in this experiment lies less in the fact that it was an independent verification of the rate constant for this very important chemical reaction but rather that this work may be a prototype of very much more selective laser temperature jump relaxation method kinetic studies of reactions in liquids.

The miniaturization of the temperature jump experiment achievable with lasers may make this a particularly. suitable technique for investigating the kinetic properties of biological cells and cell organelles.

4.7 Laser induced fusion

It is a well-known fact that tremendous amount of energy is released in fusion reaction. In the fusion reaction two light nuclei combine together to form another nucleus. The difference in mass will be converted as energy according to Albert Einstein's famous equation $E = mc^2$. Scientists have been working for the methods to generate fusion energy in a controlled manner. A thermonuclear reactor based on the laser-induced fusion is a promising method for it.

In order a fusion reaction to takes place the combining nuclei should have very high kinetic energies to overcome the Coulomb repulsive force between the protons. Very high temperatures of the order of 100 million Kelvin is required to impart such high kinetic energies to the colliding nuclei. The production of such high temperatures is one of the most important difficulties facing the controlled fusion reaction. At such high temperatures matter is completely in the ionised state, known as *plasma*. The confinement of plasma also is a serious problem. Thus, two major problems in thermonuclear fusion are (1) heating of plasmas to very high temperatures and (2) the confinement of plasmas for times long enough for substantial fusion reactions to occur. In the Russian device known as Tokamak a magnetic confinement using toroidal field is employed.

With the availability of intense laser pulses, a new idea of fusion known as **inertial confinement fusion** (**ICF**) has become emerged. It is a type of fusion energy research that attempts to initiate nuclear fusion reactions by heating, compressing and confining a fuel target, typically in the form of a pellet that most often contains a mixture of deuterium and tritium, by inertial forces which are generated when an intense laser pulse interacts with the fuel material.

To compress and heat the fuel, energy is delivered to the outer layer of the target using high-energy beams of laser light, electrons or ions, although for a variety of reasons, almost all ICF devices as of 2015 have used lasers. The heated outer layer explodes outward, producing a reaction force (inertial force) against the remainder of the target, accelerating it inwards, compressing the target. This process is designed to create shock waves that travel inward through the target. A sufficiently powerful set of shock waves can compress and heat the fuel at the center so much that fusion reactions occur.

The energy released by these reactions will then heat the surrounding fuel, and if the heating is strong enough this could also begin to undergo fusion. The aim of ICF is to produce a condition known as *ignition*, where this heating process causes a chain reaction that burns a significant portion of the fuel. Typical fuel pellets are about the size of a pinhead and contain around 10 milligrams of fuel: in practice, only a small proportion of this fuel will undergo fusion, but if all this fuel were consumed it would release the energy equivalent to burning a barrel of oil.

For laser-induced fusions the working and the power efficiency is expressed in terms of the parameter ρR, called the *areal density parameter* of the combustion in ICF, where, ρ is the density and R is the radius of the fuel pellet. Then the *burn fraction* f, which represents the Fractional burn-up of the fuel, is given by,

$$\text{Burn fraction,} \quad f = \frac{\rho R}{6+\rho R} = \frac{1}{\frac{6}{\rho R}+1} \tag{1}$$

where, the density of the fuel is measured in gm/cm^3 and the radius is measured in cm. For a 5% burn up of the fuel,

$$\frac{5}{100} = \frac{\rho R}{6+\rho R} \text{ ; Or,} \quad 30 + 5\rho R = 100\rho R$$

$$\rho R = \frac{30}{95} \approx 0.3\text{gm/cm}^2$$

As ρR increases, the denominator eqn.1 decreases and hence f increases. Let M be the mass of the fuel (deuterium-tritium) D-T pellet. We assume that it contains equal number of deuterons and tritium nuclei. [Since the masses of the D (1proton + 1neutron) and T (1 proton + 2 neutrons) are in the ratio 2:3,

$$\text{Number of D nuclei in M gm of the fuel pellet} = \frac{\frac{2}{5}M}{M_d} = \frac{\frac{2}{5}M}{2\times1.66\times10^{-24}}$$

where, M_d = 2 a m u = $2\times1.66\times10^{-24}$ gm is the mass of a deuteron. If 'f' is the burn ratio,

$$\text{Number of reactions in M gm D-T fuel} = f\,\frac{2M}{5\times2\times1.66\times10^{-24}} \tag{2}$$

The energy released in a D-T reaction is 17.6 MeV. An additional energy 4.8 MeV is released when the neutron produced during the reaction ${}_1H^2 + {}_1H^3 \rightarrow {}_2He^4 + {}_0n^1 + 17.6\text{MeV}$ is absorbed by the lithium atoms in the blanket. Therefore,

Net amount of energy released in each reaction (each deuteron) $\approx$ 22 MeV

Energy released by M gm D-T pellet = Number of reactions×energy released per reaction

$$\text{i.e.}\quad E_{output} \approx f\,\frac{2M}{5\times 2\times 1.66\times 10^{-24}}\times 22\text{ MeV} \approx f\,\frac{2M\times 22\times 10^{6}\times 1.6\times 10^{-19}}{5\times 2\times 1.66\times 10^{-24}}\text{ joule}$$

$$\approx f\,M\times 4.2\times 10^{11}\,\text{J} \tag{3}$$

Obviously,

$$\text{Mass of the spherical D-T pellet, } M = \frac{4}{3}\pi R^3\rho = \frac{4\pi}{3\rho^2}(\rho R)^3 \tag{4}$$

The temperature at which the fusion reaction will occur with high probability is ~100millionK and the kinetic energy imparted to each fuel nucleus is about 10 keV. Therefore, the

Laser energy needed for imparting 10 keV energy to one D-T pair = 2×10 keV

Laser energy needed for imparting 10 keV energy to M gm fuel pellet

= (2×10×number of D nuclei in M gm fuel) keV

$$= 2\times 10\times\frac{2M}{5\times 2\times 1.66\times 10^{-24}}\text{ keV}$$

$$= 2\times 10\times 10^{3}\times\frac{2M\times 1.6\times 10^{-19}}{5\times 2\times 1.66\times 10^{-24}}\text{ joule} \approx 4M\times 10^{8}\text{ J}$$

Since only a fraction of the laser energy is imparted to the fuel nuclei,

$$\text{Laser energy imparted to M gm fuel, } E_{laser} \approx \frac{4M\times 10^{8}}{\varepsilon}\text{ J}$$

Using eqn.4,

$$E_{laser} \approx \frac{4\times 10^{8}}{\varepsilon}\times\frac{4\pi}{3\rho^2}(\rho R)^3 \tag{5}$$

Thus, the yield ratio, Y is given by,

$$Y = \frac{E_{output}}{E_{laser}} \approx \frac{f\,M\times 4.2\times 10^{11}\,\text{J}}{\dfrac{4M\times 10^{8}}{\varepsilon}\text{J}} \approx 10^{3}\varepsilon f \tag{6}$$

Assuming $\varepsilon \approx 0.1$ and using eqn.1,

$$Y \approx 100\,\frac{\rho R}{6+\rho R} \tag{7}$$

Clearly, for Y > 1, $\rho R > 0.1$ gm/cm^2. Thus, for a sizable burn up and for a reasonable yield the value of ρR should have at least 0.2 gm/cm^2. Now, for normal D-T solid fuel, $\rho \approx 0.2$ gm/cm^3.

$$E_{laser} \approx \frac{4\times 10^{8}}{\varepsilon}\times\frac{4\pi}{3\rho^2}(\rho R)^3 \approx \frac{4\times 10^{8}}{0.1}\times\frac{4\pi}{3\times 0.2^2}(0.2)^3 \approx 3\times 10^{9}\text{ J} \tag{8}$$

This is indeed a very high value. It is obvious that, by eqn.5, for a given value of ρR, the laser energy requirement can be significantly reduced to mega-joule range by increasing the value of ρ. This can be achieved by compressing the solid fuel to densities 10^3 to 10^4 times than the normal density. There is an added advantage that at such high densities, the α-particles that are produced in the reaction, give up most their energy to the unburned fuel before leaving the pellet. This energy leads to an increased fractional burning of fuel.

The laser-induced fusion reactor

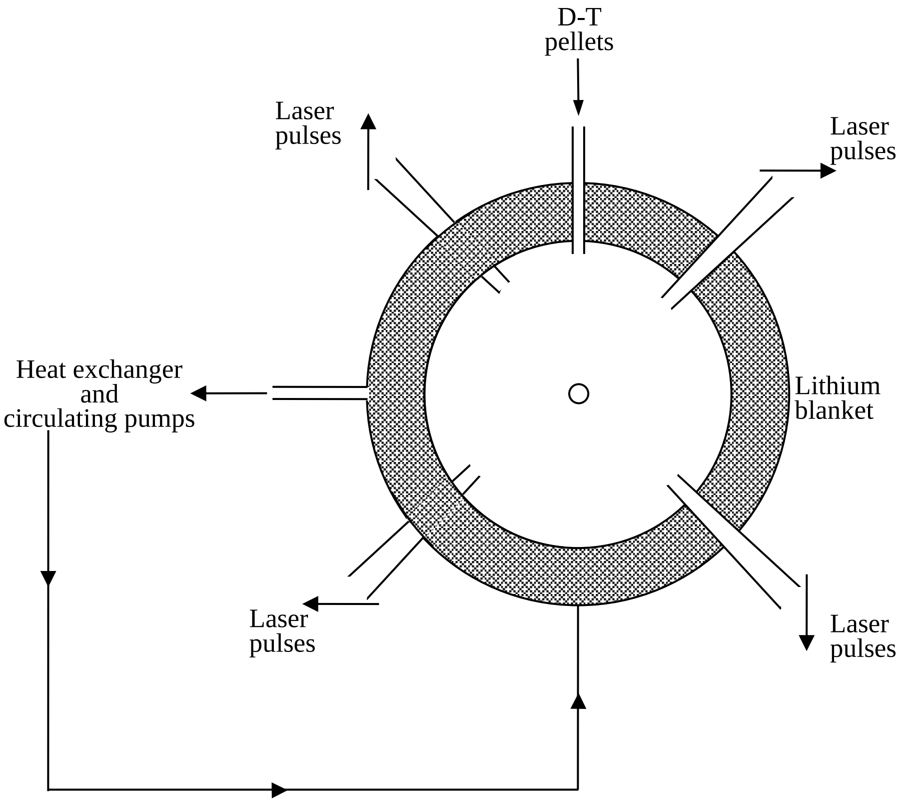

Fig.a: Schematic diagram of a D-T fusion reactor with Lithium blanket
See that laser beams are targeted to the pellet from all directions

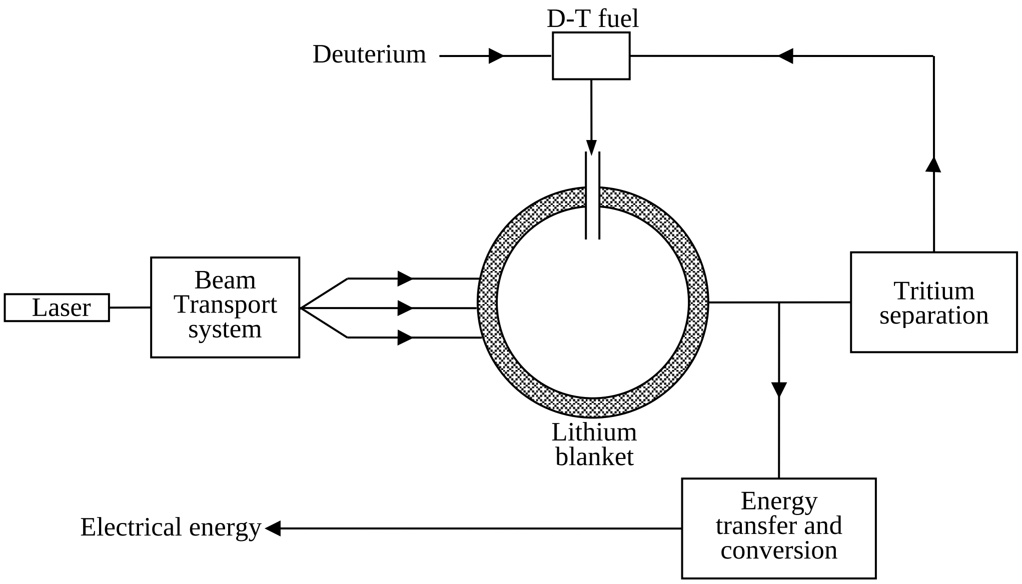

Fig.b: Block diagram of a laser-fusion electric generation system

In a laser-induced fusion reactor a D-T pellet in the form of a cryogenic solid is used as the fuel. The particle densities of the pellet are ~4×10^{22} per cm^3. It is irradiated with laser light from all directions as shown in the fig.a given below. The outer surface of the pellet is heated considerably within a short interval of time and becomes a very hot plasma with temperature ~100 million K. This hot ablation layer expands into vacuum. The reaction force gives a push to the rest of the pellet in the inward direction. Thus, if a spherical pellet is irradiated from all directions, then a spherical implosion front travels towards the core. For a D-T plasma with an incident intensity of 10^{17} W/cm^2 the inward pressure is about 10^{12} atmospheres, which is much greater than the radiation pressure about 10^8 atmospheres corresponding to this intensity. As the implosion front accelerates towards the centre, it sets up a sequence of shock waves travelling inwards which lead to a very high compression of the core and the fusion energy is released from the high compression densities along with a high temperature. In order to attain high compression densities, the time variation of the laser pulse has to be such that successive shock waves do not meet until they reach the centre of the pellet.

Fig.b is a block diagram of an electric generating station using a nuclear fusion reactor (LFR). The reactor consists of a high vacuum enclosure. The D-T pellets are dropped to the centre of the chamber at regular intervals of time. As soon as the pellet reaches the centre of the chamber it is irradiated by synchronized pulses from an array of focussed laser beams from all directions. The fusion energy released is absorbed by the walls of the chamber and this heat energy is used for running a steam turbine. For a commercial power station if 100 pellets are allowed to explode per second it produces about 10 GW (=10^{10} W).

One of the most important aspects of any fusion reactor is the production of tritium, which is not available in nature. This is achieved by placing lithium or its compound in a blanket surrounding the reactor chamber. The neutron emitted in the fusion reaction is absorbed by a lithium nucleus to give rise to tritium according to either of the following reactions.

$$_3\mathrm{Li}^6 + {}_0\mathrm{n}^1 \rightarrow {}_1\mathrm{H}^3 + {}_2\mathrm{He}^4 + 4.79\mathrm{MeV}$$

$$_3\mathrm{Li}^7 + {}_0\mathrm{n}^1 \rightarrow {}_1\mathrm{H}^3 + {}_2\mathrm{He}^4 + {}_0\mathrm{n}^1 - 2.46\mathrm{MeV}$$

Notice that in the second reaction, the neutron appears in the RHS also, which can again interact with lithium nucleus to produce tritium. In reactors liquid lithium is contained between the two structural shells which enclose the reactor cavity. The liquid lithium is also responsible for the removal of heat from the reactor and the running of the steam turbine. The heat exchangers and the tritium separation equipment are expected to be adjascent to the reactor.

*One of the earliest serious and large scale attempts at an ICF driver design was the **Shiva laser**, a 20-beam neodymium doped glass laser system built at theLawrence Livermore National Laboratory (LLNL) that started operation in 1978. Shiva was a "proof of concept" design intended to demonstrate compression of fusion fuel capsules to many times the liquid density of hydrogen. In this, Shiva succeeded and compressed its pellets to 100 times the liquid density of deuterium. However, due to the laser's strong coupling with hot electrons, premature heating of the dense plasma (ions) was problematic and fusion yields were low. This failure by Shiva to efficiently heat the compressed plasma pointed to the use of optical frequency multipliers as a solution which would frequency triple the infrared light from the laser into the ultraviolet at 351 nm. Newly discovered schemes to efficiently frequency triple high intensity laser light discovered at the Laboratory for Laser Energetics in 1980 enabled this method of target irradiation to be experimented with in the 24 beam OMEGA laser and the NOVETTE laser, which was followed by the Nova laser design with 10 times the energy of Shiva, the first design with the specific goal of reaching ignition conditions.

Fig.c: D-T Pellet

Nova also failed in its goal of achieving ignition, this time due to severe variation in laser intensity in its beams (and differences in intensity between beams) caused by filamentation which resulted in large non-uniformity in irradiation smoothness at the target and asymmetric implosion. The techniques pioneered earlier could not address these new issues. But again this failure led to a much greater understanding of the process of implosion, and the way forward again seemed clear, namely the increase in uniformity of irradiation, the reduction of hot-spots in the laser beams through beam smoothing techniques to reduce Rayleigh–Taylor instability imprinting on the target and increased laser energy on target by at least an order of magnitude. Funding for fusion research was severely constrained in the 80's, but Nova nevertheless successfully gathered enough information for a next generation machine.